Part I
Imaging and Diagnostics

Nanomaterials for the Life Sciences Vol.6: Semiconductor Nanomaterials.
Edited by Challa S. S. R. Kumar

ISBN: 978-3-527-32166-7

1
Quantum Dots for Cancer Imaging

Yan Xiao and Xiugong Gao

1.1
Introduction

Although significant progress has been made in both the understanding and treatment of cancer during the past 30 years, it remains the second leading cause of death in the United States (US). The cancer community has been called to eliminate cancer-related suffering and death by 2015, but to achieve this goal, groundbreaking innovations in both the diagnosis and treatment of cancer are needed. The noninvasive detection of cancer in its early stages is of great interest since early cancer diagnosis, in combination with precise cancer therapies, could significantly increase the survival rate of patients and eventually save millions of lives. Nanomedicine, an emerging research area that integrates nanomaterials and biomedicine, has come into the spotlight because of its potential to provide novel diagnostic tools for the detection of primary cancers at their earliest stages, and to provide improved therapeutic protocols for the effective and highly selective extermination of malignant cells. Although it could be simply described as the application of nanotechnology to medicine, nanomedicine is actually a multidisciplinary science that involves materials science, nanotechnology, physics, chemistry, biology, and medicine [1]. Research into nanomedicine will lead to the understanding of the intricate interplay of nanomaterials with components of biological systems.

Interest in nanomedicine burgeoned after the US National Institutes of Health (NIH) announced a four-year program for nanoscience and nanotechnology in medicine in December 2002 [2]. Nanoscience and nanotechnology, with their potential applications in biomedicine, have been highlighted as "Priority Areas" for funding opportunities by the National Science Foundation (NSF) since 2001 [3]. The NIH Roadmap's new Nanomedicine Initiatives, first released in late 2003, started funding a five-year plan to set up eight Nanomedicine Development Centers from 2005 [4]. To harness the power of nanotechnology to radically change the way in which cancer is diagnosed, treated and prevented, the National Cancer Institute (NCI) announced in July 2004 the Cancer Nanotechnology Plan, which

Nanomaterials for the Life Sciences Vol.6: Semiconductor Nanomaterials.
Edited by Challa S. S. R. Kumar

ISBN: 978-3-527-32166-7

is outworked by the NCI Alliance for Nanotechnology in Cancer [5]. With the grand level of attention and fervent study in the related areas, it is no longer a distant dream that nanotechnology will radically transform clinical oncology by offering high sensitivity and localized treatment for cancers with increasing variety of nanomaterials.

"Nanomaterials" is a general term used to describe structures with morphological features smaller than a one-tenth of a micrometer in at least one dimension [6]. In recent years the arsenal of nanomaterials has continued to expand, and now include seven major categories based on their composition: carbon-based nanomaterials, nanocomposites, metals and alloys, biological nanomaterials, nanopolymers, nanoglasses, and nanoceramics. On the other hand, nanomaterials can be classified according to their shape as nanoparticles, nanotubes, nanorods, or nanowires, and so on. The heart of nanomedicine lies in the ability to shrink the size of the tools and devices, based on various nanomaterials, to the nanometer size range. Indeed, the elementary functional units of biological systems – proteins/enzymes, nucleic acids (DNAs, RNAs), membranes, and many other cellular components – are all on the nanometer scale. Therefore, there are many points of intersection between nanoscience and nanotechnology and the biological sciences. It is predicted that many nanotechnologies will soon become translational tools for medicine, and move quickly from laboratory discoveries to clinical tests and therapies.

Among various nanomaterials, quantum dots (QDs) distinguish themselves in their far-reaching possibilities in many avenues of biomedicine. QDs are nanometer-sized semiconductor crystals with unique photochemical and photophysical properties that are not available from either isolated molecules or bulk solids. QD research started in 1982 with the realization that the optical and electric properties of small semiconductor particles were heavily dependent on particle size due to quantum confinement of the charge carriers in small spaces [7, 8]. During the next two decades, extensive research was carried out for potential applications in optoelectronic devices, QD lasers and high-density memory. In 1998, two seminal reports simultaneously demonstrated that QDs could be made water-soluble and could be conjugated to biological molecules, providing the first glimpse of the vast potential of QDs as probes for studying biological systems [9, 10]. In comparison with organic dyes and fluorescent proteins, QDs have the advantages of improved brightness, resistance against photobleaching, and multicolor fluorescence emission. These properties could improve the sensitivity of biological detection and imaging by at least one to two orders of magnitude. Significant improvements have been made in the synthesis, surface modification, and biofunctionalization of QDs in the following years and, indeed, the current literature is rife with examples of QDs used in various biomedical applications. It can now be said with confidence that QDs have completed the transition from a once curious demonstration of quantum confinement in semiconductors to ubiquitous fluorophores providing unique insights into biological investigations [11].

In this chapter, an attempt will be made to provide a comprehensive, state-of-the-art overview of QD applications in cancer imaging. Following a brief introduc-

tion of the topic within the broad background of biomedicine, cancer and its imaging requirements will be briefly overviewed. The following section describes the photophysics and chemistry of QDs, and a provides a clear understanding of the merits of using QDs in bioimaging, as well as the requirements and challenges in the synthesis, surface modification and bioconjugation of QDs in order to make them amenable to bioimaging applications. Next, some recent advances in the use of QDs in various imaging applications for cancer detection and diagnosis are detailed, both *in vivo* and *in vitro*. The literature cited in this section is confined to reports that are germane to cancer studies. Finally, the issue of QD cytotoxicity and potential safety concerns is briefly covered, followed by a summary of the chapter and some future perspectives on QD applications in cancer imaging.

1.2 Cancer

The word "cancer" derives from the Latin term for crab, the basis if which related to the fourteenth century when a Greek physician first used the term to describe a disease of which the swollen mass of blood vessels around a malignant tumor resembled the shape of a crab. In modern dictionaries, cancer is referred to as a malignant tumor of potentially unlimited growth that expands locally by invasion, and systemically by metastasis.

1.2.1 A Primer on Cancer Biology

Cancer is not a single disease but rather a family of different diseases. In humans, there may be more than 200 different cancers [12], based primarily on the part of the body in which the cancer first develops, referred to as the primary site. The human body, and any other multicellular organism alike, can be viewed as a society or ecosystem, the individual members of which – the cells – reproduce by cell division and organize into collaborative assemblies or tissues. Cancer is the result of mutation, competition, and natural selection that occurs in the population of somatic cells, leading to an abnormal state in which individual mutant cells not only prosper at the expense of their neighbors but also ultimately destroy the whole cellular society and die. Research has indicated that most cancers derive from a single abnormal cell, and are probably initiated by a change in the DNA sequence of that cell [13]. Cancerous cells are, on the one hand, self-sufficient in growth signals and, on the other hand, insensitive to anti-growth signals and can evade apoptosis – a process by which a cell is commanded by the environment to die [14]. As a result, these cells multiply at an exponential growth rate in an uncontrolled fashion, leading to the formation of a tissue lump called a *malignant tumor*. Gradually, the tumor tissue grows bigger and invades the adjacent tissues and organs, obstructing normal physiological functions and usually causing great pains in the patient. In many cases, the invading tumor can break loose and enter the

bloodstream or lymphatic vessels and form secondary tumors at other sites of the body – a process termed *metastasis*. The more widely a cancer metastasizes, the more difficult it becomes to eradicate. Over time, the tumor may cause malfunctioning of various organs, and ultimately proves to be fatal.

1.2.2 The Importance of Early Cancer Detection and Diagnosis

Despite rapid advances in global cancer research towards the understanding and treatment of cancer during the past several decades, the disease remains the second leading cause of death in the US, and has become the leading cause of death for patients under the age of 85 years since 1999. It is estimated that, in 2008, there will have been 1 437 180 new cases and 565 650 deaths of all cancers in the US [15]. Cancer primary sites with the highest incidence rate and/or death rate include the breast for women, prostate gland for men, and colon and rectum, lung and bronchus, non-Hodgkin lymphoma, pancreas, urinary bladder for both sexes, based on the data during the period 2000–2004 in the US [15].

The clinical outcome of cancer diagnosis is strongly related to the stage at which the malignancy is detected. The mortality of cancer would decrease substantially if it were to be detected at an early stage, when the disease could be more effectively treated. This is especially true for breast and cervical cancer in women and colorectal and prostate cancer in men. When diagnosed early, the tumor is confined to the organ of origin, and can be either resected surgically, or treated with radiation therapy and/or systemic chemotherapy. However, most solid tumors are currently detectable only after they reach a size of ~1 cm in diameter, by which time they contains millions of cells. Sadly, by this point metastasis may have already taken place so that treatment becomes much more difficult, if not impossible. The five-year relative survival rate for all cancers increased from 50% in 1975–1977 to 66% in 1996–2003 [15], due to progress in diagnosing certain cancers at an earlier stage, as well as improvements in treatment.

Cancer detection and diagnosis means an attempt to accurately identify the anatomical site of origin of the malignancy, and the type of cells involved. The most commonly used techniques in current clinical practice are tissue biopsy and medical imaging, and sometimes a bioanalytic assay of the body fluids. *Biopsy* can provide information about the histological type, classification, grade, potential aggressiveness and other information that may help to determine the best treatment regime, and also has the advantage that any tissue abnormality can be examined at the cellular level. However, biopsy is practical only if the tumor is located near the surface of the body, where a tissue sample can be easily retrieved for microscopic evaluation. When the tumor is inaccessible for a biopsy, then reliance must be placed on *medical imaging* techniques to detect the location of the tumor. Existing noninvasive imaging techniques include computed tomography (CT), magnetic resonance imaging (MRI), positron emission tomography (PET), single photon emission CT (SPECT), ultrasound, X-ray imaging, and optical imaging. These imaging methods are effective for the macroscopic visualization

of tumors and, if combined with biopsies, they are able not only to confirm the presence of tumors but also to pinpoint the primary and/or secondary sites of the lesion.

However, none of the existing techniques is sufficiently sensitive and/or specific to detect abnormalities at the microscopic level, and is thus unable to identify tumors at their incipient stage – not to mention precancerous lesions at the molecular level. In recent years, substantial research efforts have been applied to the development of better cancer imaging techniques [16], and significant progress has been seen in the development of nanoparticle-based, highly sensitive contrast agents [17]. Nanoparticle-based contrast agents such as QDs have strong potential for early cancer detection and diagnosis as they are bright and photostable, and can offer the possibility for multiplex biomarker imaging.

1.2.3 The Role of Biomarkers in Cancer Early Detection and Diagnosis

Today, it is well recognized by the cancer community that biomarkers play an increasingly important role in the effective treatment and management of cancer. *Biomarkers* are cellular indicators of physiologic state, and also of changes during a disease process. Carcinogenic transformation often results in the secretion of elevated levels of abnormal molecules or biomarkers into the body fluids, and these markers can provide information on the occurrence and progression of the disease. Many proteins have been identified as specific markers for a variety of cancers [18]. For example, serum levels of prostate-specific antigen (PSA) are elevated in prostate cancer patients, and today this is the best-known cancer biomarker in clinical use [19]. Cancer antigen (CA)-125 is recognized as an ovarian cancer-specific protein, which is present in a subset of ovarian cancer patients [20]. The identification of such biomarkers is of major interest for cancer early detection and diagnosis.

During the past few years, there has been increasing interest and enthusiasm in molecular markers as tools for cancer detection and diagnosis. Targeted cancer imaging using biomarkers is usually more sensitive and specific than nontargeted imaging. In addition, recent advances in high-throughput technologies in genomics, proteomics and metabolomics have facilitated the discovery of cancer biomarkers. These biomarkers may be genes or genetic variations, changes in mRNA and/or protein expression, post-translational modifications of proteins, or differences in metabolite levels. Some newly identified biomarkers and their use in cancer research have been described in recent reviews [21, 22]. Depending on their type, these biomarkers can be potentially useful for predicting several outcomes during the course of the disease, including risk assessment, early detection, prognosis, disease progression, recurrence prediction, and therapeutic responses. For instance, one of the most important uses of biomarkers is the classification of a specific tumor (when one has been detected) into its various subtypes since, for many cancers, each of these subtypes has a drastically different prognosis and a preferred method of treatment. In spite of the critical importance of the diagnosis

of cancer subtypes, many cancers do not yet have a reliable test to differentiate between their many different subtypes, for example, highly invasive tumors versus their less-fatal counterparts. The final judgment is usually left to the expert opinion of a pathologist who examines the tumor biopsy, with such judgment being unavoidably subjective. With the advent of high-throughput genomic and proteomic data of cancer specimen, it is becoming apparent that many cancer subtypes can be distinguished by the expression level of a specific biomarker or the expression profile of a panel of biomarkers [21].

In the pursuit of sensitive and quantitative methods for biomarker analysis, nanotechnology has been heralded as a field of great promise. Semiconductor QDs could enable the detection of tens to hundreds of cancer biomarkers in blood assays, and on cancer tissue biopsies. With the emergence of gene and protein profiling and microarray technology, the high-throughput screening of biomarkers has generated databases of genomic and expression data for certain cancer types, and this has led to the identification of new, cancer-specific markers [21]. Today, QDs are being used to expand this *in vitro* analysis and to extend it to cellular, tissue and whole-body multiplexed cancer biomarker imaging. QDs also continue to show promise in personalized medicine, which may be highly desirable to treat a patient uniquely for his or her distinct cancer phenotype [22]. Therefore, QDs bear potential impact for improving the diagnosis and treatment of cancer.

1.3 Quantum Dots: Physics and Chemistry

QDs are semiconductor nanocrystals which have a near-spherical shape and a diameter in the range of 1 to 10 nm [23]. By virtue of this nanoscale size, which is comparable to electron delocalization lengths (tens to hundreds of Angstroms), QDs possess certain unique physical properties that are unavailable in either individual atoms or bulk semiconductor solids. These properties, which are desirable for biological imaging, and when combined with the development of ways to solubilize QDs in solution and to conjugate them with biological molecules, have led to an explosive growth in their biomedical applications.

1.3.1 Photophysical Properties of QDs

In physics, solid-state materials are classified into three categories based on their electrical conductivity, namely insulators, semiconductors, and conductors. The conductivity is often rationalized as the energy difference between the valence band and the conduction band, called bandgap energy (E_g). When an electron in the valence band gains energy (either thermally or by the absorption of a photon) that is equal to or greater than E_g, it enters the conduction band, leaving behind a positively charged hole in the valence band, thus forming electron-hole pairs which are charge carriers; this process is called *excitation*. The bandgaps in semi-

conductor materials are small enough that some electrons may be excited thermally at room temperature to form charge carriers. An electron in the excited state at the conduction band may relax back to its ground state at the valence band through recombination with its hole, resulting in the emission of a photon, in the form of fluorescence, with the same energy as the bandgap E_g. Thus, the wavelength of the fluorescence emission is determined by the E_g of the semiconductor material. For bulk semiconductor materials, E_g is dictated by its composition only.

When one or more dimensions of a semiconductor are reduced under the Bohr exciton radius, which is typically a few nanometers, the so-called "quantum confinement effect" is observed [24]. The reduction of one dimension leads to a structure called a *quantum well*, where the semiconductor material is in the form of thin sheets only a few atoms thick; a reduction in two dimensions leads to the structure of *quantum wires*. When all the three dimensions are reduced to the nanometer scale, tiny spherical semiconductors – QDs – are formed. Under such situations, the bandgap energy E_g is quantized, with the value being directly related to the QD's size. In other words, the energy is no longer only a function of the semiconductor composition, but also of its size. The quantum confinement effect could be most accurately explained by quantum mechanical models, which may be enigmas for most readers with a background in biology and are certainly beyond the scope of this chapter. However, the interested reader may find in the literature a simplified explanation using the "particle in a box" analogy [25].

Due to the quantum confinement effect, it is possible to systematically control the electronic energy level spacings and, as a result, the wavelength of light emission, by adjusting the size of the semiconductor. This is the fundamental principle behind the unique photophysical properties of QDs. With different sizes and compositions, QDs can emit fluorescent light with wavelengths over a wide range spanning regions from the ultraviolet, through the visible, into the infrared [26–30] (Figure 1.1a). In addition, as QD emission is due to a radiative recombination of an exciton, it is also characterized by a long lifetime (>10 ns), and a narrow and symmetric energy band [32] (Figure 1.1b). In comparison with traditional organic fluorescent molecules, which are usually characterized by red-tailed broad emission band and short fluorescence lifetimes, QDs have several attractive optical features that are desirable for long-term, multitarget and highly sensitive bioimaging applications.

First, QDs have very large molar extinction coefficients [33], typically of the order of $0.5–5 \times 10^6\,M^{-1}\,cm^{-1}$; this is approximately 10- to 50-fold higher than those of organic dyes, which means that QDs are capable of absorbing excitation photons much more efficiently. The higher rate of absorption is directly correlated to the QD brightness, and it has been found that QDs are approximately 10- to 20-fold brighter than organic dyes [9, 10, 34]. As a result, QDs are highly sensitive fluorescent agents, allowing for the highly efficient fluorescence labeling of cells and tissues. This is of particular importance for cancer diagnosis, as many cancer biomarkers exist in low copy numbers and/or at low concentrations.

Second, QDs have excellent photostability, being typically several thousandfold more stable against photobleaching than organic dyes [35]. This feature allows the

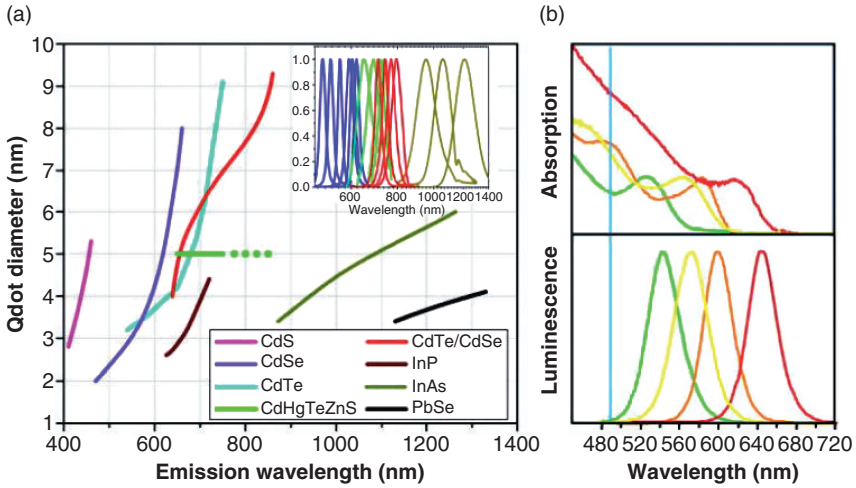

Figure 1.1 (a) Size and composition dependence of QD emission maxima. QDs can be synthesized from various types of semiconductor materials (II–VI: CdS, CdSe, CdTe ... ; III–V: InP, InAs ... ; IV–VI: PbSe ...) characterized by different bulk band gap energies. The curves represent experimental data from the literature on the dependence of peak emission wavelength on QD diameter. The range of emission wavelength is 400 to 1350 nm, with size varying from 2 to 9.5 nm (organic passivation/solubilization layer not included). All spectra are typically around 30 to 50 nm (full width at half-maximum). Inset: Representative emission spectra for some materials; (b) Absorption (upper curves) and emission (lower curves) spectra of four CdSe/ZnS QD samples. The blue vertical line indicates the 488 nm line of an argon-ion laser, which can be used to efficiently excite all four types of QDs simultaneously. Adapted from Ref. [31]; © 2005, American Association for the Advancement of Science.

real-time monitoring of biological processes over long periods of time, and is essential for cancer biomarker assays and *in vivo* imaging where much longer times are needed.

In addition, QDs have a longer excited state lifetime (20–50 ns), which is about one order of magnitude longer than that of organic dyes [32]. This allows the effective separation of QD fluorescence from background fluorescence by using a time-gated or time-delayed data acquisition mode [36]. In this mode, signal acquisition is not started until the background autofluorescence disappears largely, since this way the signal-to-noise ratio (SNR) will be increased dramatically, resulting in a significantly improved image contrast [37, 38]. Therefore, QDs are highly suitable for time-correlated lifetime imaging spectroscopy.

Moreover, QDs have broad absorption bands, narrow emission bands, and a large Stokes shift (Figure 1.1b). Unlike organic dyes, the excitation and emission spectra of QDs are well separated. Depending on the wavelength of the excitation light, the Stokes shift of QD may be as large as 400 nm, and this allows further improvement of detection sensitivity in imaging tissue biopsies and living organisms [39]. Biological specimens contain a variety of intrinsic fluorophores such as proteins and cofactors, yielding a significant background signal that decreases

probe detection sensitivity. The peak of the intrinsic fluorescence falls in the blue to green spectral region. Due to the broad absorption band and the large Stokes shift, QDs can be tuned to emit with longer wavelengths in the red or infrared spectra, where autofluorescence is diminished.

Lastly – and most importantly – the wavelength of QD emission is size-tunable, which is a unique feature of QD materials in comparison with organic dyes. The size-dependent emission of QDs allows the imaging and tracking of multiple targets simultaneously, using a single excitation source. This is of particular importance in cancer detection and diagnosis, since it has been realized that a panel of disease-specific molecular biomarkers can provide more accurate and reliable information with regards to the disease status and progression than can any single biomarker [21]. Although theoretically possible, the multiplexing of QD signals would not be practically feasible without the combination of their characteristic broad absorption bands and narrow emission bands. While broad absorption bands allow multiple QDs to be excited with a single light source of short wavelength – thus simplifying instrumental design and increasing detection speed – their narrow emission bands (as small as 20 nm in the visible range) allow for distinct signals to be detected simultaneously, with very little overlapping (Figure 1.1b). In stark contrast, organic dyes and fluorescent proteins have narrow absorption bands but relatively wide emission bands, rendering the detection of separated signals from distinct fluorophores more difficult.

1.3.2 Quantum Dot Chemistry

The development of QD-based fluorescent probes involves a multistep process that includes synthesis, surface passivation, solubilization, and bioconjugation.

1.3.2.1 Synthesis

QD crystals are composed of hundreds to thousands of atoms that typically belong to Group II and VI elements (e.g., CdSe, CdTe, ZnSe) or Group III and V elements (e.g., InP and InAs) in the Periodic Table. Among the various synthetic methods that have been reported, two are most popular. Early studies used aqueous-phase synthesis in reverse micelles; this produces water-soluble QDs but they are usually of low quality [40]. In order to produce high-quality QDs, later studies used a method in which the synthesis was carried out at an elevated temperature in an organic solvent, and this has now becomes the most widely used technique of synthesizing highly homogeneous and highly crystalline QDs. The solvent is nonpolar with a high boiling point, and is most commonly a mixture of trioctylphosphine, trioctylphosphine oxide (TOPO), and hexadecylamine, all of which have long alkyl chains [26, 41, 42]. The purpose of using hydrophobic organic molecules as mixed solvents is two-fold. First, the mixture serves as a robust reaction medium, and second, their basic moieties also coordinate with unsaturated metal atoms on the QD surface to prevent the formation of bulk semiconductors. As a result the ligand alkyl chains are directed away from the QD surface, forming

a highly hydrophobic monolayer that is only soluble in nonpolar solvents such as chloroform and hexane.

1.3.2.2 Surface Passivation

The QD nanocrystal core (e.g., CdSe) is often coated with a shell of a wider bandgap semiconductor material (e.g., ZnS or CdS). This process, which often is called *surface passivation*, is extremely important as it serves multifold purposes [43, 44]. First, it protects the core from oxidation, and prevents the leaching of highly toxic Cd^{2+} ions. More importantly, it drastically improves the quantum yield by reducing surface defects and thus preventing nonradiative decay. Nonradiative recombination events occurring at surface defects decrease fluorescence efficiency. Due to the large surface-to-volume ratio of QD nanoparticles, surface-related recombination resulting from the localized trapping of carriers is considered to be one of the main factors that reduce the emission efficiencies of QDs [45]. The use of a higher bandgap semiconductor as a passivation shell confines the charge carriers to the core QD, thus minimizing surface recombination and leading to a significant improvement (up to >50%) in fluorescence quantum yields [44]. CdSe is normally passivated with ZnS, resulting in a structure referred to as (CdSe)ZnS or CdSe/ZnS, but ZnSe and CdS are also commonly used [44, 46, 47].

1.3.2.3 Water Solubilization

QDs produced using most of the synthesis strategies (especially the hot solvent method) are water-insoluble. For biological applications, these hydrophobic particles must first be rendered hydrophilic so that they are soluble in aqueous buffers. Two general strategies have been developed for the surface modification (Figure 1.2), namely ligand or cap exchange, and native surface modification by amphiphilic polymer coating [48].

In ligand or cap exchange the hydrophobic ligands on the QD surface are replaced with bifunctional ligands such as mercaptoacetic acid or mercaptosilane [9, 10]. The bifunctional ligands have two moieties, one which binds strongly to the QD surface (e.g., thiol), and the other which points out from the QD surface, forming a hydrophilic shell (e.g., hydroxyl, carboxyl). This method, which often is called "cap exchange," has two disadvantages: (i) an increased tendency to form particle aggregation, thus decreasing fluorescent efficiency; and (ii) an increased potential toxicity due to the exposure of toxic QD elements as a result of desorption of labile ligands from the QD surface.

In native surface modification, the native hydrophobic ligands (e.g., TOPO) are retained on the QD surface, but an amphiphilic polymer is introduced to interact favorably with the hydrophobic alkyl chains, while simultaneously leaving the hydrophilic segment directed away from the QD surface, thus rendering the QDs water-soluble. Several such polymers have been reported, including octylamine-modified polyacrylic acid [49], polyethylene glycol (PEG)-derivatized phospholipids [50], block copolymers [39], and amphiphilic polyanhydrides [51]. As the original hydrophobic ligands (TOPO) are retained on the inner surface of QDs, the QD core is shielded from the outside environment by a hydrocarbon bilayer. Thus,

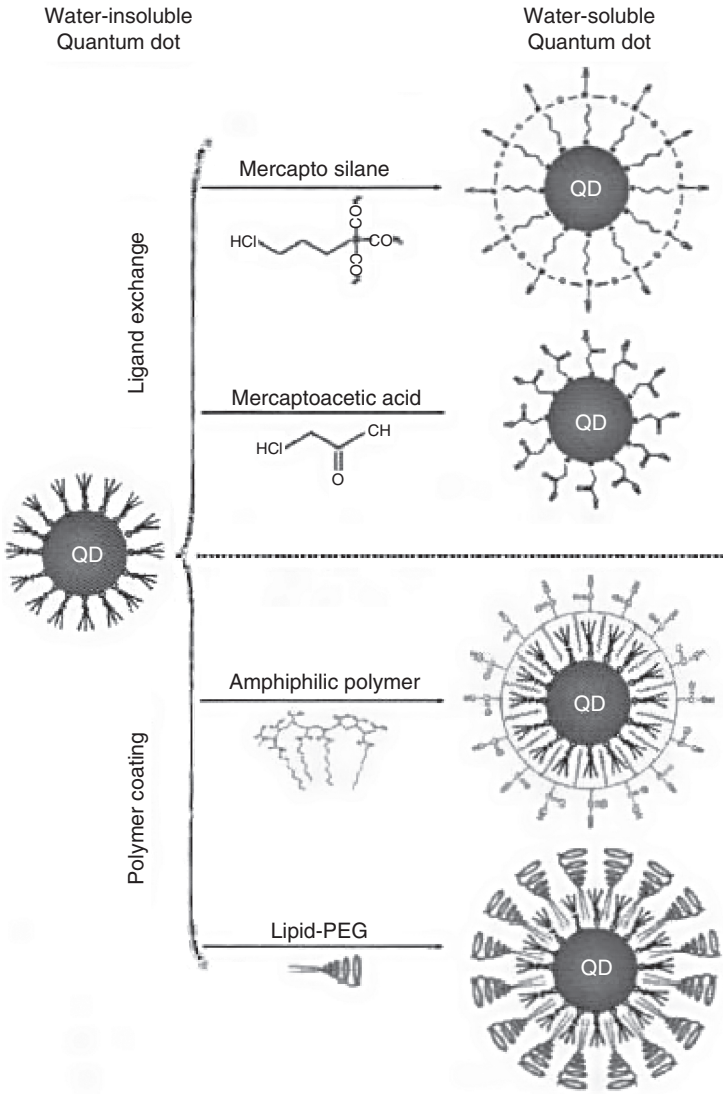

Figure 1.2 Diagram of two general strategies for phase transfer of TOPO-coated QD into aqueous solution. The ligands are drawn disproportionately large for detail, but the ligand-polymer coatings are usually only 1–2 nm in thickness. The top two panels illustrate the ligand exchange approach, where TOPO ligands are replaced by heterobifunctional ligands such as mercapto silanes or mercaptoacetic acid. This scheme can be used to generate hydrophilic QD with carboxylic acids or a shell of silica on the QD surfaces. The bottom two panels illustrate the polymer coating procedure, where the hydrophobic ligands are retained on the QD surface and rendered water soluble through micelle-like interactions with an amphiphilic polymer or lipids. From Ref. [48]; © 2007, Springer-Verlag.

this latter method is more advantageous than the first at maintaining the QD optical properties and storage stability in aqueous buffer over a broad range of pH and salt concentrations [39], as well as having a reduced cytotoxicity [51], but unfortunately increases the overall size of the QD probes. To date, however, this is the preferred procedure for the commercial production of water-soluble QDs.

1.3.2.4 **Bioconjugation**

For biological applications such as cellular imaging, QDs must be conjugated to biomolecules (e.g., proteins, antibodies, peptides, DNA, etc.), and for this several approaches have been developed (Figure 1.3) [52]. A commonly used strategy is to use QDs that contain streptavidin, which provides a convenient and indirect link to a variety of biotin-tagged biomolecules [49, 53–56] (Figure 1.3a). However, since the streptavidin-biotin complex is quite bulky, in cases where QD particle size is a consideration, for example when intracellular pores have to be crossed or cellular transport proteins are targeted, small covalent linkages are often preferred. As most solubilization methods results in QDs capped with ligands containing

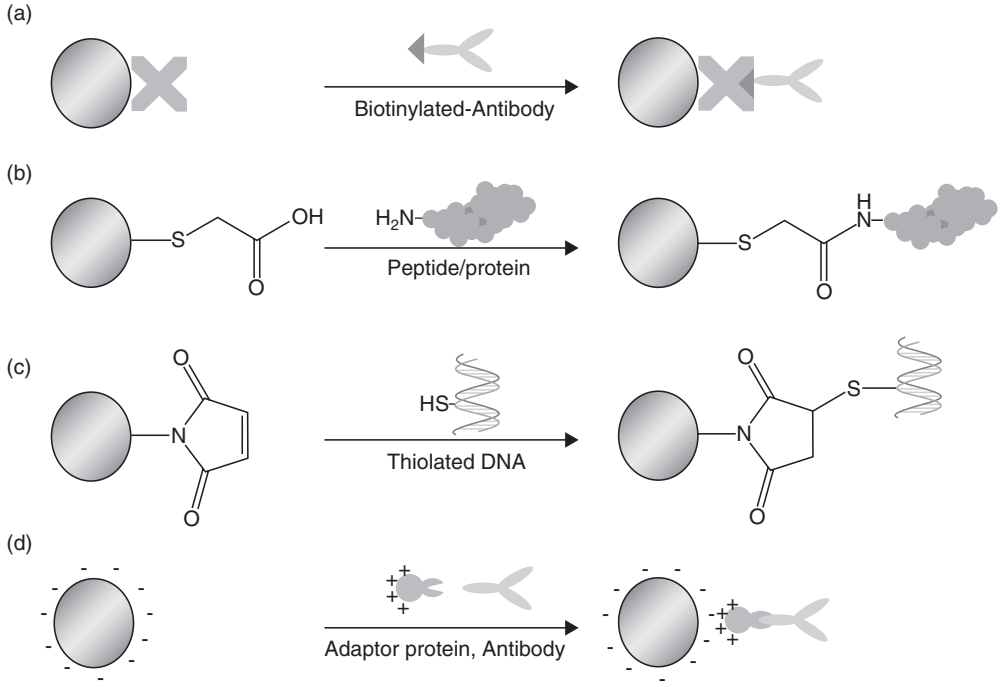

Figure 1.3 Examples of the bioconjugation of differently functionalized QDs to biomolecules by various strategies. (a) Streptavidin and biotin affinity binding; (b) Amide bond formation between carboxylic acid groups on QD surface and amine groups on proteins; (c) Thioether bond formation between maleimide groups on QD and thiol groups on thiolated DNA; (d) Electrostatic interaction between negatively charged QDs and positively charged biomolecules. From Ref. [52]; © 2007, Elsevier Inc.

hydrophilic groups such as carboxylic acids and maleimides, biomolecules containing basic functional groups such as amines and thiols can form stable amide or thioether bonds directly with QDs (Figure 1.3b,c) or through heterobifunctional crosslinkers [10, 49, 50, 57–60]. QDs in aqueous buffer solutions are negatively charged; therefore, positively charged molecules, such as cationic avidin proteins or recombinant maltose-binding proteins fused with positively charged peptides, could be conjugated to QDs through electrostatic interactions [53, 61–63] (Figure 1.3d). More detailed reviews on this topic can be found elsewhere [31, 52, 64].

It should be pointed out that none of these methods can control the number of proteins per QD. There is also a lack of experimental tools to control the orientation of a protein immobilized on the QD surface. For specific targeting, it is highly desirable that the delivery proteins (e.g., antibody) are properly oriented and fully functional. Goldman *et al*. first explored this area by using a fusion protein as an adapter for immunoglobulin G antibody coupling to QDs [63]. The adapter protein has a protein G domain for binding to the antibody Fc region, and a positively charged leucine zipper domain for electrostatic interaction with negatively charged QDs. As a result, the Fc end of the antibody is attached to the QD surface, leaving the target-specific $F(ab')_2$ domain facing outwards. As the bioconjugation step is critical to the success of bioimaging, the surface engineering of QD nanoparticles represents a field that will require much further study in the future.

1.4
Cancer Imaging with QDs

Bioconjugated QD fluorescent probes offer a promising and powerful imaging tool for cancer detection and diagnosis. Their much greater brightness, rock-solid photostability and unique capabilities for multiplexing, combined with their intrinsic symmetric and narrow emission bands, have made them far better substitutes for organic dyes in existing diagnostic assays. Following the two seminal reports in *Science* during 1998, demonstrating the feasibility of using QDs in biological environments [9, 10], many new techniques have been developed during the past decade, utilizing the unique photophysical properties of QDs, for the *in vitro* biomolecular profiling of cancer biomarkers, *in vivo* tumor imaging, and dual-functionality tumor-targeted imaging and drug delivery (Table 1.1). Some of these emerging technologies are currently being improved and integrated into clinical practice in oncology, and may have important implications for the diagnosis, prognosis, and therapeutic management of cancer patients in the near future.

1.4.1
In Vitro Screening and Detection of Cancer Biomarkers Using Microarrays

As the clinical outcome of cancer patients is heavily dependent on the stage at which the malignancy is detected, early screening is extremely important in any type of cancer. Techniques currently available in clinical practice for cancer

Table 1.1 Summary of quantum dots applications in cancer imaging.

Imaging type	Applications		References
In vitro	High-throughput screening and detection of cancer biomarkers	Profiling cancer biomarker expression on tissue microarrays (TMAs)	[65–67]
		Cancer biomarker detection in fluidic biological specimens using microarrays	[68, 69]
	Cellular labeling of cancer biomarkers	Cancer biomarker labeling by immunohistochemistry (IHC) in fixed cells and tissue sections	[49, 66, 70–85]
		Cancer genetic mapping by fluorescence *in situ* hybridization (FISH)	[84, 86–91]
	Live cell imaging	Labeling and imaging of cell-surface receptors in cancer cells	[49, 54, 70, 81, 92–100]
		Labeling and imaging of intracellular targets in cancer cells	[10, 101–129]
In vivo	*In vivo* tracking of cancer cells	Cancer cell tracking for homing, migration, engrafting, and metastasis potential.	[39, 114, 115, 130, 131]
	Tumor vasculature imaging	Nontargeted imaging of tumor vasculature	[130, 132]
		Targeted imaging of tumor vasculature	[133, 134]
	Sentinel lymph node (SLN) mapping	SLN mapping in tumor-bearing animals	[135–137]
		Fluorescence lymphangiography for studying the lymphatic drainage networks	[138, 139]
	Whole-animal tumor imaging	Targeted molecular imaging of tumors in animals	[39, 60, 100, 107, 125, 133, 140–143]
		Nontargeted imaging of tumors in animals	[130, 144]

Table 1.1 *Continued*

Imaging type	Applications		References
Multimodality	Positron emission tomography (PET)	Dual-modality imaging probe for both NIR fluorescence imaging and PET	[145, 146]
	Magnetic resonance imaging (MRI)	Dual-modality imaging probe for both NIR fluorescence imaging and MRI	[147, 148]
Multifunctionality	Drug delivery	QD-based nanoparticles for imaging and drug delivery	[107, 149]
	Small interfering RNA (siRNA) delivery	QD-based nanoparticles for imaging and siRNA delivery	[128, 150]

diagnosis such as medical imaging and tissue biopsy are neither highly sensitive nor highly specific for the detection of cancers at their incipient stage. In comparison, cancer screening and diagnosis using molecular biomarkers is usually more sensitive and specific, and is at the same time less invasive, less laborious, and less expensive. There is also a growing belief that a panel of markers rather than one marker alone will predict a more accurate outcome. Herein, lies the great potential offered by QDs, which can be used as sensitive probes for the screening and detection of cancer markers in clinical specimens. The intense and stable fluorescent properties of QDs, coupled with their multiplexing capacity, could enable the screening and detection of tens to hundreds of cancer biomarkers in *in vitro* diagnostic assays, promising for rapid and accurate clinical diagnostics.

In theory, QDs are particularly well suited to microarray applications, especially when multiplexing is needed. However, in most array applications developed to date, organic fluorescent dyes such as Cy3, Cy5, fluorescein isothiocyanate (FITC) and the Alexa series were used. One possible reason for this lies in the fact that array imaging is less demanding on fluorescence stability, by virtue of the high-speed laser scanners used. Nonetheless, it has been shown that Alexa Fluor 488 faded quickly during laser scanning cytometry (LCS) rescanning, with only 75% fluorescence intensity remaining after five scans; in contrast, QDs remained almost unchanged (98%) after the same number of scans [86].

During the past few years, many reports have been made where QDs were used as fluorescence probes in array imaging. Among these, several have been related to cancer biomarker identification and detection [65–69]. Ghazani *et al.* first demonstrated the use of QD bioconjugates as fluorescence probes for profiling the protein expression of tumor antigens on tissue microarrays (TMAs) [65]. Multiplexed staining with QDs of different emission spectra allowed the simultaneous

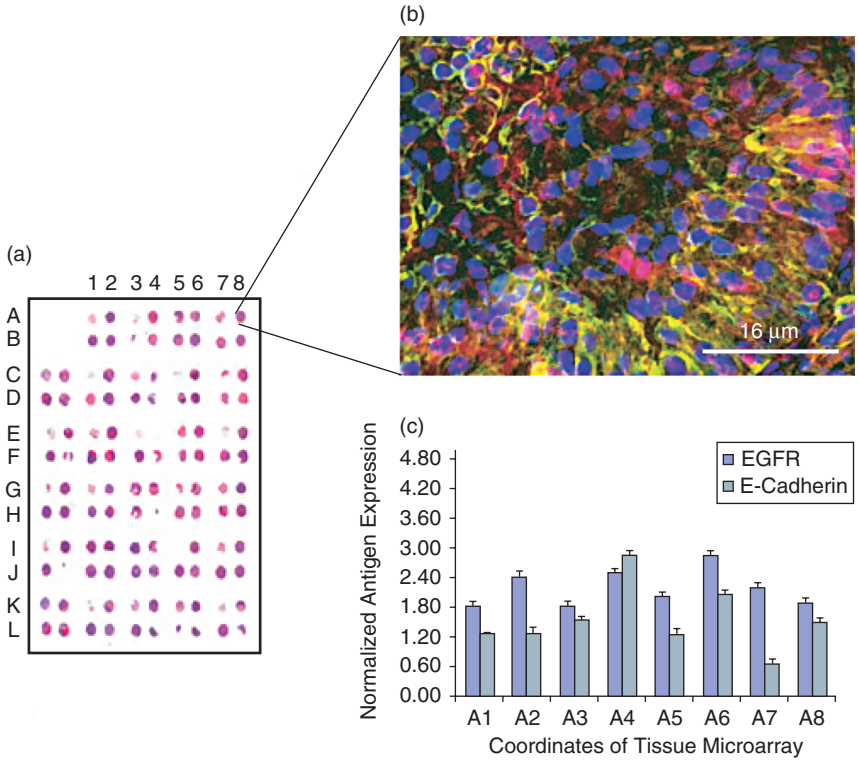

Figure 1.4 Quantification analysis of cancer-derived antigens in tissue microarray. (a) Tissue cores on a tissue microarray (hematoxylin and eosin image) were stained for EGFR, cytokeratin, and E-cadherin; (b) The fluorescent image (40×) is a composite picture of the antigens detected by individual QD immunostaining (of different color emission) for each of the targets. 4′,6-diamidino-2-phenylindole (DAPI) staining is used to locate nuclei in blue; (c) The antigen (EGFR and E-cadherin) expression values (normalized to cytokeratin) in each lung cancer xenograft cores. From Ref. [65]; © 2006, American Chemical Society.

detection of epidermal growth factor receptor (EGFR), E-cadherin, and cytokeratin on formalin-fixed and paraffin-embedded (FFPE) A549 lung carcinoma tissue sections (Figure 1.4). In this study, the use of QDs in conjunction with optical spectroscopy provided a tool to obtain a sensitive, accurate and quantitative measurement on a continuous scale that was not attainable by using traditional methods. Subsequently, QD-based tissue microarrays have been used successfully to distinguish tumor tissues from normal tissues in clinical samples [66, 67]. Zajac *et al.* developed a QD-based microarray platform that is potentially useful for cancer biomarker detection in fluidic biological specimens such as serum, plasma, and body fluids [68]. For this, the QDs were conjugated to the detector antibody either directly or via streptavidin–biotin interaction. In a series of multiplexing experiments, these authors were able to detect six different cytokines down to picomolar

concentrations, thus demonstrating the high sensitivity of the QD-based detection system. In another study, Gokarna *et al*. reported the fabrication of QD-based protein biochips for the detection of the prostate cancer biomarker, PSA [69]. Here, the QDs were conjugated directly to anti-PSA antibodies in order to minimize any nonspecific binding, while retaining the high affinity of the QD bioconjugates. With an array spot size down to the nanometer scale, the authors were able to demonstrate the potential of nanoarrays for the detection of biomolecular interactions at the molecular level.

Although published reports in this area are sparse, the results of these studies have proved that QDs are highly promising for the high-throughput sensitive and specific detection of cancer biomarkers, and will undoubtedly inspire further investigation in the near future that, ultimately, will lead to efficient the *in vitro* screening and detection of various types of cancers.

1.4.2 *In Vitro* Cellular Labeling of Cancer Biomarkers

Determination of the expression and spatial distribution of molecular biomarkers in patient tissue specimens has substantially improved the pathologist's ability to classify disease processes. Many disease pathophysiologies, including cancers, are marked by the characteristic increased or decreased expression of certain biomarkers. Diagnostic and prognostic classifications of human tumors are currently based on immunohistochemistry (IHC) or fluorescence *in situ* hybridization (FISH), both of which have been used for almost a century. However, traditional IHC or FISH is mostly qualitative rather than quantitative, and is consequently subjective to an individual pathologist's bias. Moreover, traditional methods using organic dyes have a single-color nature and are unable to perform the multiplexed detection of several biomarkers simultaneously. In recent years, QDs have been used successfully in place of organic dyes in IHC and FISH analysis for labeling cancer biomarkers in fixed cells or tissue specimens. In many cases, the quantitative and simultaneous profiling of multiple biomarkers has been achieved by virtue of their intense and stable fluorescence, coupled with their multiplexing capacity. In addition, QDs have been applied successfully to live cell labeling for basic biological studies, as well as for developing clinically relevant applications for cancer detection and therapy.

1.4.2.1 Labeling of Fixed Cells and Tissues

The application of bioconjugated QDs for specific cancer biomarker labeling by IHC was first reported in 2003, when Wu *et al*. used QDs to label the breast cancer marker HER2 on the surface of SK-BR-3 cells, and in tissue sections from mouse mammary tumors [49]. These authors showed the labeling signals to be specific for the intended target, and to be brighter and considerably more photostable than comparable organic dyes. These results indicated that QD-based probes could be very effective in cellular imaging, and offered substantial advantages over organic dyes in multiplex target detection. This study was the first step towards using

QD-based diagnostics to help guide therapeutic decisions for cancer patients. Subsequently, many different cellular biomarkers, both general and/or specific to various cancers, have been labeled using QDs in fixed cells and tissues, including HER2 [49, 66, 70–73], estrogen receptor (ER) [71, 73] and EGFR [71] for breast cancer, CA125 for ovarian cancer [74], PSA for prostate cancer [75], (potentially useful) biomarkers of risk for colorectal cancer [76], tumor vasculature cluster of differentiation (CD) markers [77, 78], cytokeratin 18 on ovarian tumors [78], adrenocorticotropic hormone (ACTH) in pituitary adenoma [71], as well as mortalin [79], *p*-glycoprotein [80], carcinoembryonic antigen (CEA) [81], telomerase [66] and tumor-associated carbohydrate antigens [82] that each have differential expression levels and/or expression patterns in various cancer cells in comparison with normal cells. These studies have made it clear that QD are superior to organic dyes for cellular biomarker labeling in fixed cells and in FFPE tissue sections of tumor biopsies.

As no single biomarker can effectively predict all stages of cancer, an accurate diagnosis and prognosis of cancer must rely on a suite of several markers. Therefore, there is a growing need for multiplex staining due to the limited quantity of clinical samples. The optical properties of QDs have engendered considerable interest in their application to multiplex IHC for the simultaneous identification and colocalization of multiple biomarkers. By using QDs with different emission spectra, the practicality of the simultaneous detection of two cellular targets with one excitation wavelength was first demonstrated by Wu *et al*. [49]. In this case, HER2 on the cell surface and nuclear antigens in the nucleus of SK-BR-3 cells were detected simultaneously with QDs of different wavelengths conjugated to different secondary detection reagents. Subsequently, Kaul *et al*. studied the subcellular distribution of two heat-shock proteins, mortalin and heat-shock protein (HSP) 60, by double-labeling cells with red- and green-emission QDs, respectively [83]. These authors were able to visualize minute differences in the subcellular niche of these two proteins in normal and cancer cells. Fountaine *et al*. reported that five different cellular markers could be analyzed simultaneously on the same section of routinely processed FFPE tissues by using QDs with distinct emission spectra [77]. Later, Bostick *et al*. described a QD-based IHC system that could detect, simultaneously, up to six biomarkers that were potentially useful for predicting the risk of colorectal cancer [76]. Itoh *et al*. simultaneously detected two breast cancer biomarkers, HER2 on the cell membrane and ER in the nucleus, in human breast tissues [71]. These authors showed that very weak signals produced by conventional immunofluorescence and/or enzyme-labeled antibody methods could be significantly enhanced using QD labeling. Very recently, Xu *et al*. also reported the simultaneous detection of HER2 and ER in FFPE human breast cancer tissue using QDs emitting at 550 and 610 nm [73]. Sensitive spectra and images obtained in this study made possible the quantitative measurement of subcellular proteins inside the tumor tissues. Whilst all of the above-described reports on multiplex labeling have relied on sequential staining, which is both time-consuming and laborious, Sweeney *et al*. have recently developed a single-step, multiplex staining method in which streptavidin-conjugated QDs are conju-

gated to biotinylated primary antibodies; this enabled the multiplexed labeling of up to three cellular biomarkers on FFPE samples [78]. Shi *et al.* also reported the concurrent staining of three proteins in fixed cells [75].

Although the high intensity and photostability of QDs make the quantitative analysis of immunofluorescence signals possible, until now QD-based IHC for cancer biomarker detection has been mostly qualitative, with very few studies having attempted the quantitative analysis of biomarker expression [70, 73, 75, 76, 78]. Robust quantitation allows biomarker validation, as well as an accurate diagnosis of cancer progression, and to this end the present authors' group has been investigating the development of a quantitative IHC imaging system that combines the advantages of QD fluorescence imaging with the high sensitivity and specificity of IgY antibodies developed for cancer biomarkers. As a consequence, the relative quantitation of cancer biomarkers HER2 and telomerase has been demonstrated in tissue microarrays of patient and control tissues [66] (Figure 1.5a). Although the patient numbers were small, the study demonstrated the feasibility of the relative quantitation of cancer biomarkers with IgY and QD fluorophores, and showed promise for rigorous clinical validation in large patient cohorts. By using SK-BR-3 and MCF-7 as reference control cell lines, this assay platform allows for the accurate quantitative measurement of HER2 expression in breast cancer specimens [84]. Karwa *et al.* also reported quantitative multiplexed detection of inflammation biomarkers in tissue sections using QD conjugates where the quantitation of biomarker expression by fluorescence intensity correlated well with clinical disease severity in a mouse colitis model [85].

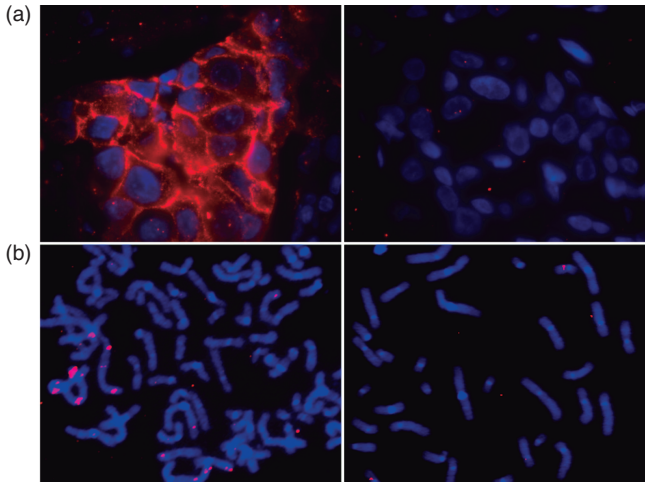

Figure 1.5 (a) Immunohistochemistry detection of breast cancer biomarker HER2 with anti-HER2 IgY antibody and QD fluorophores in breast cancer TMA sections with HER2 overexpression (left) and with normal HER2 expression (right); (b) FISH with BAC CTD-2019C10 probe and QD fluorophores for *HER2* gene amplification detection in fixed cell culture of breast cancer SK-BR-3 cells (left) and of normal PB-6 cells (right).

Today, FISH is used routinely in research and clinical laboratories for applications such as gene mapping, quantitation of gene copy number in tumors with gene amplification, or quantitation of the density of telomere repeats at the ends of human and mammalian chromosomes. Unfortunately, reports on the use of QDs (conjugated to oligonucleotide probes) as fluorescent tags in FISH have been relatively few in number, reflecting the technical difficulties of this endeavor, such as the optimization of QD/oligonucleotide conjugation, signal stability, tissue autofluorescence, and quantitation of signal. Initially, it was shown that QD fluorescent tags were better than standard FISH for detecting *HER2* oncogene amplification in breast cancer cells, by showing that fluorescence from QD fluorophores was significantly brighter and more photostable than the organic fluorophores Texas Red and fluorescein [87]. In this experiment, biotinylated DNA probes were detected using streptavidin-conjugated QDs (Figure 1.5b), and it was also shown that pH of the final incubation buffer had a significant effect on the fluorescence of QD-detected hybridization signals in the FISH experiments [86]. Coupled with the use of control cell lines, this method promises the accurate determination of *HER2* gene copy number in fixed cells and FFPE tissue samples [84].

In order to allow for the detection of multiple genes by exploiting the multiplexing capability of QDs, the labeling of DNA probes directly by QDs is required, and this has since been demonstrated in several studies [88–90]. For this, a faster, single-step FISH protocol was employed which coupled hybridization with detection and eliminated the need for any laborious secondary amplification. Chan *et al*. directly labeled oligonucleotide probes by QDs through streptavidin and biotin interactions, and used the probes for the simultaneous study of the subcellular distribution of multiple mRNA targets in mouse brain sections [88]. Bentolila *et al*. developed direct QD-probes by attaching short DNA oligonucleotides onto QDs and using the probes to target repetitive satellite noncoding DNA sequences [89]. In order to improve probe sensitivity and specificity, Jiang *et al*. used large genomic DNA probes directly labeled with QDs to visualize gene amplification in the cells of lung cancer specimens [90]. The results of these studies have suggested that the QD-FISH probes may offer an effective approach to analyze cancer-related genomic aberrations in basic research and clinical applications. More recently, Byers *et al*. developed a multiplex QD-based FISH that was both semiautomated and quantitative, and could be applied to the high-throughput processing of FFPE tissue samples [91]. The use of spectral imaging for the detection and subsequent deconvolution of multiple signals has also enabled the sensitive colocalization of multiple genes, and facilitated the quantitation of fluorescence signals from each gene.

Interestingly, both Chan *et al*. [88] and Byers *et al*. [91] combined QD FISH with QD IHC in the same experiment, which facilitated the simultaneous study of multiple mRNA and protein markers in tissue culture and histological sections.

1.4.2.2 **Live Cell Imaging in Cancer Cells**

Live cell imaging with QDs can provide information that is not possible with imaging in fixed cells, such as monitoring several intercellular and intracellular

interactions in real time over a period as long as several days. On the other hand, the imaging of live cells is a more challenging task than imaging fixed cells, in that care must be taken to keep the cells alive, and that efficient methods are required to deliver QD probes across the cell membrane for imaging intracellular targets. Moreover, it has been commonly observed that QDs tend to aggregate in the cytoplasm and are often trapped in endocytotic organelles such as endosomes, lysosomes, and other intracellular vesicles. Nevertheless, significant progress has been made during the past few years in the use of QDs as fluorescent probes for labeling and imaging cell-surface proteins as well as intracellular proteins in live cells.

1.4.2.2.1 **Labeling and Imaging of Cell-Surface Receptors** Imaging membrane receptors on the cellular surface is relatively easier than imaging those inside the cells, as these proteins can often be labeled using techniques similar to those used for fixed cells through antibody–antigen or receptor–ligand interactions. Considerable success has been achieved in using QD bioconjugates as imaging agents for the specific targeting and imaging of cellular surface antigens on live cancer cells. Wu *et al.* first demonstrated the use of QD–streptavidin conjugates as probes together with Herceptin (a humanized anti-HER2 antibody) and biotinylated goat anti-human IgG, for the specific detection of HER2 on the surface of live SK-BR-3 cells [49]. Lidke *et al.* coupled QDs directly to epidermal growth factor (EGF), a small protein with a specific affinity for the erbB/HER receptors. After adding the EGF-QDs to cultured human cancer cells, it was possible to observe EGF binding to the receptor and subsequent internalization of the receptor conjugate in real time, at the single-molecule level [54]. Minet *et al.* used a QD–streptavidin conjugate and biotinylated concanavalin A (ConA) to image glycoproteins on the plasma membrane, in order to study the microdosimetry of heat stress in a tumor model of breast cancer cells [92]. QD fluorescence from labeled cells allowed the observation of alterations in plasma membrane organization and integrity as a result of the thermal effects from the heat stress. These applications have inspired the subsequent use of QDs for monitoring various plasma membrane proteins such as EGFR [93–96], G-protein-coupled receptors [97], prostate-specific membrane antigen (PSMA) [98], transferrin receptor [99], CEA [81], and dansyl (DNS) receptors [100].

The live cell labeling of membrane proteins by QDs may have implications for important biological applications. The dynamics of membrane proteins in living cells has become a major issue to understand important biological questions such as chemotaxis, synaptic regulation, or signal transduction. QDs have opened new perspectives for the study of membrane properties, as they enable measurements at the single molecule level with a high SNR. Li-Shishido *et al.* labeled HER2-overexpressing human breast cancer cell line KPL-4 with QDs conjugated to anti-HER2 antibody Herceptin, and traced the movement of the QDs on the cell membrane over periods up to 50 s, during which 2500 images were taken and subsequently superimposed [70]. Traces of centers of fluorescence spots from the superimposed images showed the detailed movement of the QDs (Figure 1.6).

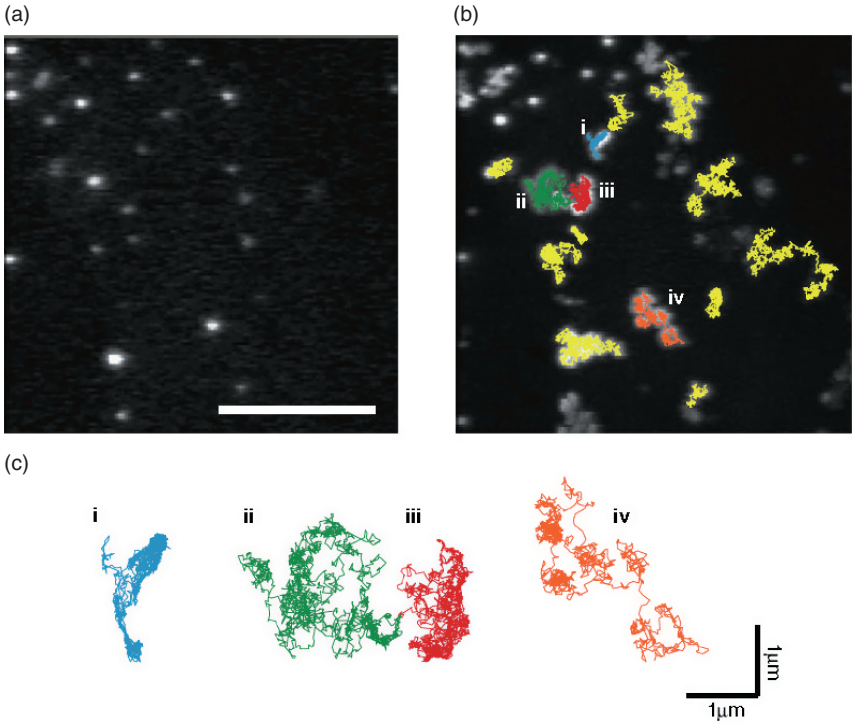

Figure 1.6 Movement of the QDs on the cell membrane. QDs labeled with anti-HER2 antibody (Herceptin) were bound to living KPL-4 cells overexpressing HER2. (a) Fluorescence images of QDs were taken under a total internal reflection microscope at an exposure time of 20 ms and laser power of ~70 W mm^{-1} [2]. Scale bar = 5 μm; (b) The QDs bound to cells were taken at a higher magnification. To trace the movement of QDs, 2500 images were collected over a 50 s period and then superimposed. Colored lines indicate the traces of single QDs; (c) Traces indicate movements of QDs that occurred on the cell membrane for a 50 s period. Adapted from Ref. [70]; ©, 2006 Elsevier Inc.

This study also opens up the application of QDs as tools for nanometer-scale measurements of positions.

1.4.2.2.2 **Labeling and Imaging of Intracellular Targets** The first problem to tackle for the intracellular imaging of live cells using QD bioconjugates is how to circumvent the plasma membrane barrier. Several strategies have been employed for the delivery of QD probes across the membrane into cancer cells:

1. **Receptor-mediated endocytosis.** In the seminal studies of Chan and Nie [10], QDs were conjugated to transferrin and spontaneously entocytosed by HeLa cells. This receptor-mediated endocytosis mechanism was used in several subsequent studies [101–107]. By targeting receptors that are overexpressed specifically on the surface of cancer cells, but not on normal cells, QDs can be selectively delivered into tumor cells [108, 140, 151]. However, a recent study

has indicated that QDs may have severe consequences on cell physiology, as it was found that QDs coupled to ligands such as transferrin can be arrested within endosomes and somehow perturb the normal endosomal sorting in cells [106].

2. **Spontaneous endocytosis.** Many cell types are also able to engulf QDs spontaneously through nonspecific uptake [109–111, 152]. It has been noted that the surface chemistry of QDs has profound effects on their cellular uptake [112]. In addition, differences in cancer cell phenotypes can lead to significant differences in the intracellular sorting, trafficking, and localization of QDs [113].

3. **Chemical-mediated transfection.** QDs can be delivered into intracellular spaces by attaching to cationic lipids [114–116] or cationic cell-penetrating peptides such as polyarginine and Tat [117–120], or being encapsulated within a lipid emulsion [153]. The mechanism of Tat-mediated cellular uptake of QD bioconjugates has recently been studied systematically in living cancer cells under different endocytosis-inhibiting conditions [121]. The results suggest that Tat-QDs internalize through lipid-raft-dependent macropinocytosis, which is different from that of Tat conjugates with organic dyes such as FITC.

4. **Microinjection.** QDs can be delivered into the cytoplasm of a single cell through microinjection [122]. This technique is obviously useful for studying single cells, but it is labor-intensive and requires the delicate manipulation of one cell at a time. Therefore, it is difficult to obtain statistically relevant data because of the small number of cells that could be realistically injected.

Several new methods have also been developed in recent years for the intracellular delivery of QD bioconjugates. Kaul *et al.* used internalizing antibodies against mortalin/HSP70, a member of the heat-shock protein family that has a dynamic subcellular distribution, as QD caters for the active delivery of QDs into live cancer cells [123]; the molecular mechanism of this internalization has yet to be resolved, however. QD-based mortalin staining can be used to study senescence in cancer cells [124]. The specific intracellular uptake of QD-antibody conjugates by pancreatic cancer cells [103], liver cancer cells [125] and mesothelioma cells [126] has also been reported. A novel method for the intracellular delivery of QDs to image subcellular structures in live cells has been reported recently by Kim *et al.* [127]. For this, QDs conjugated to antibodies were first incorporated into biodegradable polymeric nanospheres. Then, upon cellular internalization, the pH-dependent reversal of surface charge of the nanospheres enabled their escape from the endolysosomal compartments to the cytoplasmic space, where a controllable release of the functionalized QD probes could be achieved through hydrolysis of the polymeric capsule. By attaching QDs of different emission spectra to antibodies against varying cellular targets, the multiplexed labeling of subcellular structures inside live cells was also demonstrated [127]. This approach allowed the noninvasive, high-throughput cytoplasmic delivery of QDs, with minimal toxicity to the cell. Yezhelyev *et al.* designed a QD-based nanoparticle with

proton-absorbing polymeric coatings (proton sponges) on the QD surface for the efficient delivery of QDs bound with small interfering RNA (siRNA) into the cytoplasm [128].

It is interesting to note that Zhang *et al.* have demonstrated a potentially useful method for the specific delivery of QDs into cancer cells by using the protease-modulated cellular uptake of QD conjugates [129]. Here, the QDs were conjugated to cationic peptides which were in turn linked to blocking peptides through a linker peptide (protease substrate). The negatively charged blocking peptides could then prevent the cationic peptide-mediated cellular uptake of the QD conjugates. As proteases such as matrix metalloproteases (MMPs) are greatly involved with tumor formation and progression in many types of human cancers, the overexpression of these proteases in cancer cells can remove the negatively charged groups by enzymatic hydrolysis of the linker peptide, leading to uptake of the QD conjugates specifically into cancer cells. Modulation of the uptake of nanoparticles into cells with tumor-specific enzymes may lead to a selective accumulation of nanoparticles in tumor cells, a procedure which may in time find wide applications in nanomedicine.

QD-based fluorescent probes for intracellular labeling and imaging has been instrumental in basic biological studies, such as the molecular mechanisms of intracellular transport process involving motor proteins. Nan *et al.* measured the motions of the motor proteins kinesin and dynein along microtubules by following the movements of endocytic vesicles that contain QDs [117]. By virtue of the exceptional brightness and photostability of the QDs, it was possible to record individual microtubule motor steps with 300 μs time resolution and 1.5 nm spatial precision. These studies demonstrated the ability of QDs to probe the operation of motor proteins at the molecular level in living cells, under physiological conditions. While the calculation used in this study was based on two-dimensional (2-D) trajectories of QD-containing vesicles, a more recent investigation conducted by Watanabe *et al.* involved monitoring the stepwise movements generated by myosin, dynein, and kinesin in three dimensions [102]. By using QDs conjugated to HER2 and a three-dimensional (3-D) confocal microscope, it was possible to watch the QD-enclosing vesicles (after they had been endocytosed into the cells) be moved along the membrane by transferring actin filaments, along microtubules toward the nucleus, or away from the nucleus back to the cell membrane, and with time resolution and spatial precision similar to those reported in the previous study. This study added further information towards an understanding of the molecular mechanisms underlying traffic to and from cellular membranes. By using dual-focus imaging optics, the time interval between data points of the displacements may be as short as 2 ms [104]. Very recently, the same group used QD bioconjugates to study intracellular protein movement over long periods of time and showed that, in contrast to the smoothly continuous movement of kinesin found in *in vitro* assays, kinesin in live cells displayed a "stop-and-go" behavior, where kinesin came to an almost stop, paused for a few seconds, and then moved once again. The maximum velocity of kinesin observed in live cells was also faster than that in the *in vitro* assays [116].

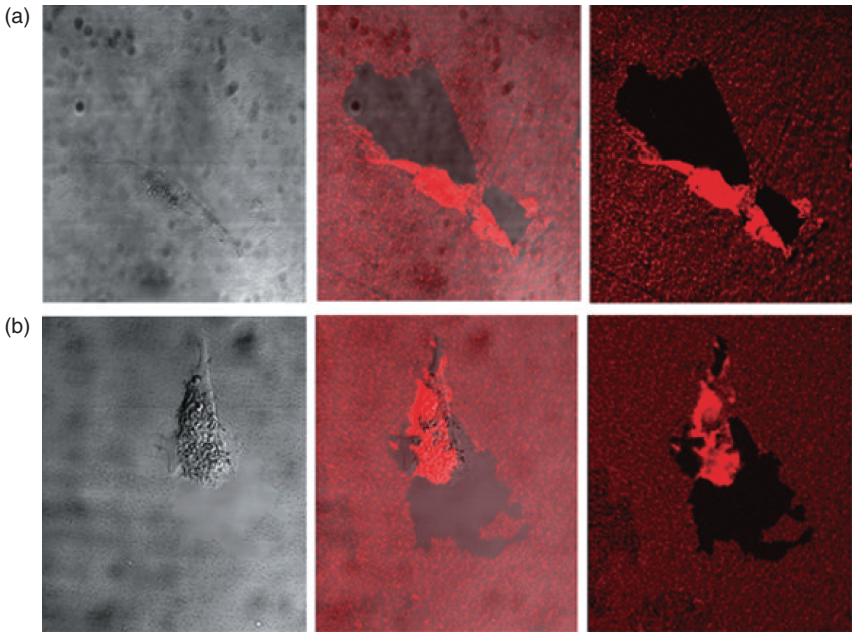

Figure 1.7 Phagokinetic tracks of the highly metastatic human mammary gland adenocarcinoma cell line MDA-MB-231 (a) and the human mammary ductal carcinoma cell line MDA-MB-435S (b) grown on a collagen substrate that had been coated with a layer of silanized, water-soluble QDs Images were collected with a confocal microscope using a fluorescence detector to record the nanocrystal trails (right) and a transmitted light detector to visualize the cells (left); the merged pictures (middle) colocalize the cells and the layer. After 24 h, sizable regions free of nanocrystals, larger than the cells themselves, were detected. From Ref. [109]; © 2003, International Society of Differentiation.

Some of the QD applications for intracellular targeting and imaging are also relevant to clinical cancer diagnosis and drug discovery. One such application is the cell motility assay developed by Alivisatos and colleagues [109–111], in which the migration of cells over a homogeneous layer of QDs was measured in real time. As the cells moved across, they endocytosed the QDs and, as a consequence, left behind a fluorescence-free trail (Figure 1.7). By subsequently determining the ratio of cell area to fluorescence-free track area, it was possible to differentiate between invasive and noninvasive cancer cells. As the motility of cancer cells *in vitro* is strongly correlated with their metastatic potential *in vivo*, this assay method could aid in the clinical classification of cancers for better diagnosis and management. In another application, Chen *et al.* coupled QDs to molecular beacons (MBs) to measure the expression of the endogenous proto-oncogene *c-myc* in MCF-7 breast cancer cells [122]. MBs are retained in the cytoplasmic compartment after being linked to QDs. Consequently, false-positive signals are reduced to marginal levels, as such nonspecific signals only arise in the nucleus of living cells. By quantifying the total fluorescent signal emanating from individual cells, accurate

measurements of RNA expression of the oncogene at the single-cell level were made possible. Garon *et al*. used QDs attached to membrane-translocating peptides to label hematologic cells in malignant and nonmalignant patient samples [120], and showed that the QD-peptide conjugates could be taken up by a diverse range of hematologic cells, and followed through many divisions and through differentiation. Taken together, these results establish QDs as extremely useful molecular imaging tools for the study of hematologic cells. Yet another clinically relevant application was developed by Wylie *et al*., of a multiplexed assay to determine the effects of drugs on different cell lines in high-throughput format [118]. By labeling live cells with QDs of different emission spectra and identifying cell proliferation using a microplate cytometer, it was possible to determine the differential rates of cell proliferation of the individual cell lines in the same well over time. Determining the differential responses of normal cells compared to cancerous cells in response to a chemical stimulus by using this assay method might prove valuable in selecting compounds that have maximal antitumor activity, while incurring minimal toxicity to normal tissues.

1.4.3 *In Vivo* Cancer Imaging

The visualization of tissue, with its anomalies, can provide information that allows certain pathologies to be eliminated, and the most probable pathology to be diagnosed. In today's oncological investigations, *in vivo* imaging can provide such a large amount of information that diagnoses are subject to much less uncertainty, and clues are also provided for the optimization of treatment. Some of the major imaging techniques used routinely in hospital set-ups for cancer diagnosis include CT, MRI, PET, SPECT, ultrasound and X-ray imaging. These techniques rely on signals that can transmit through thick tissue, and generate image contrast from the differences in signal attenuation through different tissue types. As tumors differ from normal tissues in both their structure and anatomy, many tumors can be identified based on the image contrast generated with or without exogenous contrast agents. However none of these modalities has a sufficiently high spatial resolution that is capable of detecting cancers at early stages, when the size of the tumors is very small. Moreover, most of these techniques are very expensive.

Optical imaging–particularly fluorescence imaging–is a sensitive and relatively inexpensive imaging technique that has higher intrinsic spatial resolution and for which the potential for cancer diagnosis has been demonstrated in living animal models [154, 155]. In contrast to *in vitro* fluorescence microscopic studies on cell cultures or thin tissue sections, *in vivo* fluorescence imaging functions at a macroscopic level on the whole body of animals. Whilst this enables the visualization of biology in its intact and native physiological state, it also presents some technical challenges. For example, thick, opaque animal tissues absorb and scatter photons and generate a strong autofluorescence, all of which obscure signal collection and quantification [156]. In order to overcome these problems, the near-infrared (NIR) optical window (650–950 nm) can be exploited for deep-tissue optical imaging

[157]. This is because the penetration of NIR light into tissue is significantly higher than light of shorter wavelengths, as the Rayleigh scattering decreases with increasing wavelength, and most tissue chromophores have a weak absorption in the NIR range. In recent years, several organic dyes have become available that can be used as NIR probes for *in vivo* imaging [155], but unfortunately these suffer from the same photobleaching problems as their visible counterparts. QD emission wavelengths can be tuned throughout the NIR spectrum by adjusting their composition and size; this results in photostable NIR-emitting QDs that can greatly expand their potential for *in vivo* cancer imaging. Consequently, by using appropriate hardware and software, multispectral imaging or spectral unmixing can be achieved so that the signal degradation caused by autofluorescence can be removed while adding enhanced multiplexing capabilities [39, 73, 77, 114, 158–160].

1.4.3.1 *In Vivo* Tracking of Cancer Cells

Cell tracking has the goal of determining the fate of a particular cell population within a heterogeneous environment. Cancer cell tracking can provide information on the homing, migration and engrafting of tumor cells, and thus further the current understanding of the critical stages of cancer pathology, such as metastasis. The unique photophysical properties of QDs make them desirable for the long-term tracking of cancer cells *in vivo*, and to this end the cancer cells can be labeled with QDs *in vitro*, administered to animals, and then followed using fluorescence microscopy. As an example, Gao *et al.* labeled human cancer cells with QDs and injected the cells subcutaneously into an immunecompromised mouse [39]. Subsequent *in vivo* whole-animal imaging indicated that, whilst a subcutaneous deposit of ~1000 QD-labeled cancer cells could be easily visualized, green fluorescent protein (GFP) stably transfected cells could not be detected under the same conditions. Voura *et al.* used QDs to track metastatic tumor cell extravasation *in vivo*. For this, melanoma cells labeled with QDs were injected intravenously into mice, and followed as they were extravasated into the lung tissues. The QDs and spectral imaging allowed the simultaneous identification of five different populations of cells using multiphoton laser excitation [114]. This approach allowed the study of single cells at the early stages of metastasis, and the process to be examined at the single-cell level in a natural tissue environment. A simultaneous identification and study of the interactions of multiple different populations of tumor cells and tissue cells within the same animal was also possible.

The homing mechanism of bone marrow-derived cells, and their contribution to tumor neovascularization, have been the subjects of intense debate [161]. Indeed, there has been a general paucity of such information obtainable from *in vivo* cell tracking studies. To this end, Stroh *et al.* successfully monitored the recruitment of QD-labeled bone marrow-derived precursor cells to the tumor vasculature [130]. Here, the cells were labeled *ex vivo* with QDs and imaged *in vivo* as they flowed, rolled over, and adhered to tumor blood vessels following intravenous administration (Figure 1.8). *In vivo* cell tracking studies can also aid in the behavioral profiling of cancers. It has been revealed from outcome studies of many types of cancer, that tumors of indistinguishable histologic appearance may differ

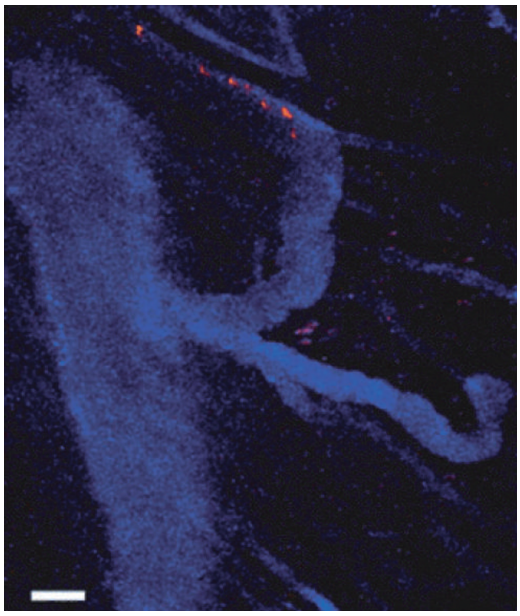

Figure 1.8 Tracking of QD-labeled bone marrow-derived precursor cells to the tumor vasculature. Seven images are superimposed in time as a single bone marrow lineage-negative cell labeled with QD590-Tat (orange) navigated the tumor vessels highlighted with QD470 micelles (blue) *in vivo*. The image represents seven repeated scans at a fixed depth (~100 µm) taken at 1 s intervals. Scale bar = 50 µm. Adapted from Ref. [130]; © 2005, Nature Publishing Group.

significantly in their degree of aggression and in their response to therapy. To enable an early identification of patients at high risk for disease progression, and to allow for the screening of multiple therapeutic agents simultaneously for their efficacy, Estrada *et al.* developed an orthotopic organ culture model of bladder cancer to obtain quantitative measurements of tumor cell behavior [131]. For this, human transitional cell carcinoma cells were first labeled with QDs; the cells were then instilled into the rat bladder *in vivo*, after which the bladder was excised and cultured *ex vivo*. By monitoring cell implantation, proliferation, and invasion into the organ wall, it was possible to assign distinct phenotypes to two metastatic bladder cancer cell lines, based on their different patterns of invasiveness into the bladder wall. These findings suggest that this assay system could recapitulate the salient aspects of tumor growth in the host, and be amenable to the behavioral profiling of human cancer.

Recently, Chang *et al.* reported using lipid-enclosed QDs as contrast agents to track tumor cells in a subcutaneous mouse model with epi-detection third harmonic generation (THG) microscopy [115]. Here, the QDs were mixed with a mixture of lipids to form a cationic lipid coating in order to improve their solubility and cell uptake. The epi-THG intensities were 20-fold stronger than the corresponding fluorescence intensities which, when combined with a high-

penetration 1230 nm laser, provided a method that would allow for cell tracking in deep tissues.

Surface coatings on QDs may sometimes render them too large to enter into cells, unless they are taken up by naturally occurring internalization mechanisms (e.g., phagocytosis). To facilitate cell labeling, one solution to this problem is to couple the QDs to targeting molecules that facilitate cellular uptake; examples are Tat peptide [39, 130] and the proprietary Q-Tracker from Invitrogen [162]. Negatively charged QDs can also be efficiently transduced into tumor cells using cationic lipids [114, 115]. Recent studies of cell-penetrating surface coatings have offered promise for additional solutions to this problem [163]. The encapsulation of QDs in the internal aqueous phase of lipid bilayer vesicles (liposomes) to form QD–liposome hybrid nanoparticles might offer yet another solution to the problem. More recently, Al-Jamal *et al.* showed that such QD–liposome hybrids, when injected intratumorally into solid tumor models, led to an extensive fluorescence staining of tumor cells compared to injections of QDs alone [164]. These hybrid nanoparticles constitute a versatile tool for the very efficient labeling of cells both *ex vivo* and *in vivo*, and particularly when long-term imaging and tracking of cells is sought. Moreover, such a system offers many opportunities for the development of combinatory imaging and therapeutic modalities by incorporating both drug molecules and QDs within the different compartments of a single vesicle.

1.4.3.2 **Tumor Vasculature Imaging**

Cancerous cells can induce capillary (blood vessel) growth in the tumor by secreting various growth factors such as vascular endothelial growth factor (VEGF). This process, termed *tumor angiogenesis*, is believed not only to supply the required nutrients that allow for tumor expansion, but also to serve as a waste drainage, removing the biological end-products from rapidly dividing cancer cells. Angiogenesis is also required for the spread of a tumor, or metastasis. Consequently, the noninvasive imaging of tumor angiogenesis has many clinical applications, including lesion detection, patient stratification, new drug development and validation, treatment monitoring, and dose optimization.

Several reports have been made during the past few years using QDs as a contrast agent for the nontargeted imaging of normal vascular systems in small animals. Foe example: Larson *et al.* showed that green-light emitting QDs remained both fluorescent and detectable in the capillaries of adipose tissue and the skin of a live mouse following intravenous injection [165]; Lim *et al.* used NIR QDs to image the coronary vasculature of a rat heart [166]; and Smith *et al.* imaged the blood vessels of chicken embryos with a variety of NIR and visible QDs [167]. Recently, Jayagopal *et al.* demonstrated the potential for QDs to serve as molecular imaging agents for targeted vascular imaging [168]. For this, spectrally distinct QDs were first conjugated to antibodies against three different cell adhesion molecules (CAMs), and then injected intravenously into a rat model of diabetes. Fluorescence angiography of the retinal vasculature revealed CAM-specific increases in fluorescence, and allowed imaging of the inflammation-specific behavior of

individual leukocytes as they floated freely in the vessels, rolled along the endothelium, and underwent leukostasis. The unique spectral properties of QDs allowed the simultaneous imaging of up to four spectrally distinct QD tags. It was also found in this study that, by incorporating PEG crosslinkers and Fc-shielding antibody fragments into the QD–antibody conjugates, their *in vivo* circulation times and targeting efficiency could be increased.

In 2005, two groups reported the use of QDs for the nontargeted *in vivo* imaging of tumor vasculature in mice. Morgan *et al.* coated NIR QDs with bovine serum albumin (BSA) and injected them either subcutaneously or intravenously into mice bearing murine squamous cell carcinoma (SCC). This allowed the blood vessels surrounding and traversing a SCC tumor that was growing in the right hind leg of a C3H mouse, and which had a diameter on the order of ~100 μm and was located at a depth of several hundred microns, to be clearly visualized [132]. These data showed that the QDs represent a valuable angiographic contrast agent for blood vessels surrounding and penetrating the tumor tissues. Stroh *et al.* used PEG-coated QDs and two-photon microscopy to image blood vessels within the microenvironment of subcutaneous tumors in mice, and to concurrently image and differentiate tumor vessels from both the perivascular cells and the matrix through green fluorescent protein (GFP) in the perivascular cells and autofluorescence from collagen in the extracellular matrix (ECM). A stark contrast between the cells, ECM, and the erratic, leaky vasculature was evident [130]. Taken together, the results of these studies pointed towards the use of QDs as fluorescence contrast agents for the high-resolution, noninvasive imaging of tumor vasculatures.

The first attempt to use QD for the targeted *in vivo* imaging of blood vessels in tumors was reported by Cai *et al.* [133]. For this, NIR QDs labeled with arginine-glycine-aspartate (RGD) peptide were used for the active targeting and imaging of blood vessels expressing $\alpha_v\beta_3$ integrins in a murine xenograft model of subcutaneous human glioblastoma tumors. The tumor location could be identified by virtue of the specific binding of the RGD-labeled QDs to the tumor vasculature. More recently, Smith *et al.* used the same methodology to target RGD-labeled QDs to newly formed/forming blood vessels expressing $\alpha_v\beta_3$ integrins in a SKOV-3 ear tumor mouse model [134]. By using high-resolution (~0.5 μm) intravital microscopy, it was possible to observe the binding of QD conjugates to the tumor blood vessels, with details at the cellular level (Figure 1.9). These authors showed that the QDs did not extravasate, but bound as aggregates rather than individually; the latter finding was of critical relevance to the regulatory approval of nanoparticles in human clinical applications for disease diagnostics and therapeutics, as concerns have been expressed that the aggregation of QDs might contribute to their cytotoxicity. The RGD–QD conjugates used in these studies were prepared from commercially available PEG-coated QDs and thiolated RGD peptides through a heterobifunctional linker, 4-maleimidobutyric acid *N*-succinimidyl ester [169]. It has been suggested recently that peptides containing isoaspartate-glycine-arginine (*iso*DGR) may also be conjugated to QDs as binding ligands for the targeted imaging of tumor vasculature [170].

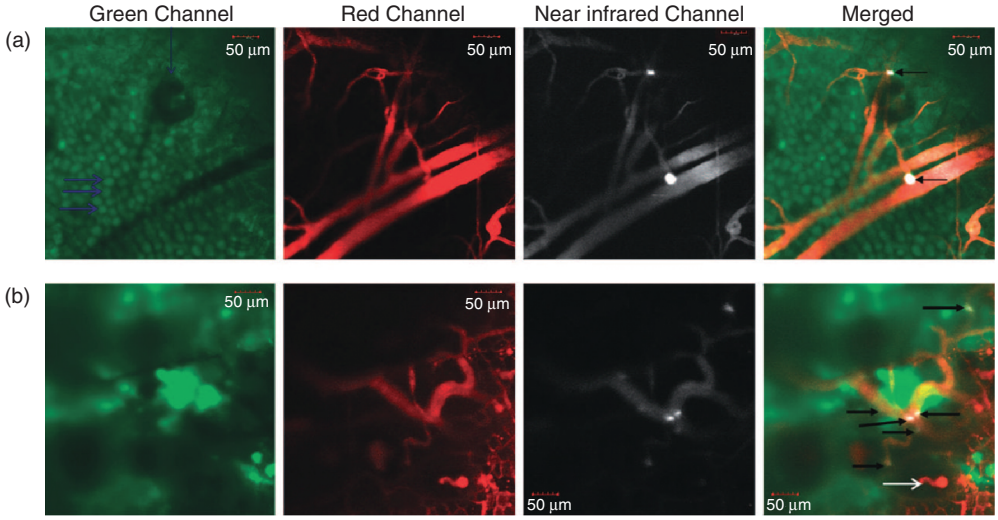

Figure 1.9 Direct visualization of binding of RGD-QDs to tumor vessel endothelium. (a) These panels display different output channels of the identical imaging plane along the row with scale bars. In the green channel, individual EGFP-expressing cancer cells are visible (marked by thick horizontal blue arrows; the vertical blue arrow points to a hair follicle), while the red channel outlines the tumor's vasculature via injection of Angiosense dye. The NIR channel shows intravascularly administered QDs which remain in the vessels (i.e., they do not extravasate). Binding events are visible by reference to bright white signal. These are demarcated by arrows in the rightmost merged image, in which all three channels have been overlaid; (b) These panels display the same as panels (a) in a different mouse, except that a sixfold higher RGD-QD dose has been injected. Individual cells are not generally visible. Six binding events are observed in this field-of-view, as marked by arrows in the merged image at right. White arrows in the bottom merged image designate areas of tissue autofluorescence. Adapted from Ref. [134]; © 2008, American Chemical Society.

1.4.3.3 Sentinel Lymph Node Mapping and Fluorescence Lymphangiography

Sentinel lymph node (SLN) mapping has revolutionized the intraoperative staging of many solid tumors, and is now the standard of care in breast cancer and melanoma [171]. The underlying hypothesis of SLN mapping is that sampling of the first lymph node to receive lymphatic drainage from a solid tumor is sufficient to assess for the presence or absence of lymphatic metastasis [172]. If no malignant cells are found in the SLN, the patient is spared the morbidity of radical lymph node dissection. The current clinical practice of SLN mapping is performed with a combination of preoperative radiocolloid injection and intraoperative injection of a visible blue dye. Unfortunately, this procedure suffers from the drawbacks of potential radiation hazards, along with the extra cost of the radioisotope, allergic reactions after blue dye injection, the overall long duration of the procedure, and technical difficulties in performing the mapping. In particular, the blue dye used for locating the SLN is extremely difficult to see in the presence of blood or anthracosis. Thus, technological innovation is clearly needed.

NIR QDs have innate features that make them an excellent choice as lymphatic tracers for SLN mapping. Most QDs have a hydrodynamic diameter in the range of 10–20 nm and a negatively charged coating, which not only allows them to undergo rapid uptake into lymphatics but also provides them with excellent retention in the lymph nodes. The NIR emission permits fluorescence detection from deep inside the tissue, with a low background autofluorescence. Frangioni and colleagues have pioneered the use of QDs for NIR fluorescence SLN mapping, by using an imaging system that simultaneously displays color video and NIR fluorescence images. In this way, these authors have shown that QDs can be used for real-time intraoperative imaging of SLN in the skin [173], breast [173], lung [174], esophagus [175], pleural space [176], small intestine [177, 178], stomach [178], and colon [178] in small animals (mouse, rat), and also in large animals approaching human size (e.g., pigs). Although these studies did not incorporate a model system with spontaneous cancer metastatic to regional lymph nodes, they have shown that QD-mediated SLN mapping overcomes the limitations of currently available methods, permits patient-specific imaging of lymphatic flow and sentinel nodes, and provides highly sensitive, real-time *in situ* visual guidance for cancer surgery that would enable surgeons to identify and excise nodes draining from primary metastatic tumors, both quickly and accurately. More recently, the value of this technology for SLN mapping in tumor settings has also been demonstrated in pigs with spontaneous melanoma [135] and in mice bearing subcutaneous tumors [136, 137]. Here, the hydrodynamic diameter of QDs was found to have a profound impact on the tracer behavior *in vivo*, with the average time for QDs to be detected in SLN after injection increasing in line with the increasing QD diameter [135, 137].

The multiplexing capabilities of QDs can also be exploited for fluorescence lymphangiographic studies of the lymphatic drainage networks. Due to their small size and poor access, the lymphatic system has been difficult to study *in vivo*, especially when mapping lymphatic drainage simultaneously from multiple basins. However, by injecting QDs of different colors at two different locations, Hama *et al*. were able to observe the QDs draining to a common node, using wavelength-resolved spectral fluorescence lymphangiography [138]. In a subsequent study, the same group demonstrated the simultaneous visualization in real time of five separate lymphatic flows *in vivo* and their trafficking to distinct lymph nodes, using QDs with similar physical sizes but different emission spectra [139] (Figure 1.10). These studies have important implications for predicting the route of cancer metastasis into the lymph nodes.

Robe *et al*. recently studied the selective accumulation of QDs in axillary lymph nodes, and their biodistribution in different tissues in mice [179]. Here, the QDs were detected in the nodes as soon as 5 min and up to 24 h after the injection. Maximum amounts of QDs in the nodes were detected at 60 min after injection, and this corresponded to 2.42% of the injected dose. Most of the injected QDs remained at the injection site, with none being detected in other tissues, nor in the plasma, urine, and feces.

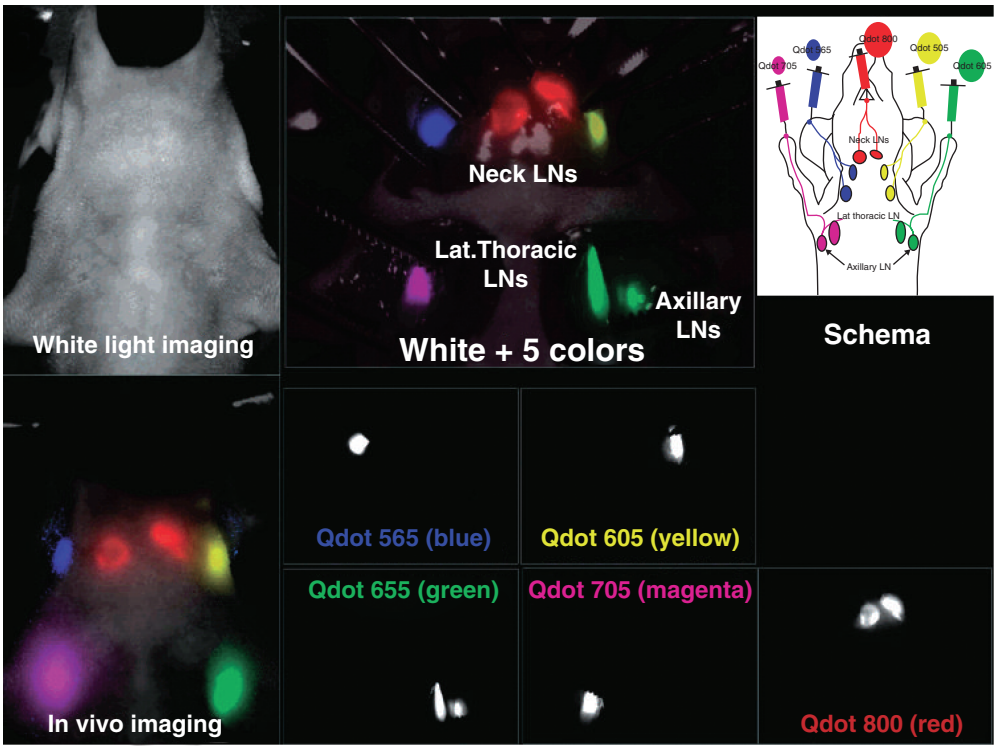

Figure 1.10 *In vivo* five-color lymphatic drainage imaging showing five distinct lymphatic drainages of a mouse injected with five carboxyl QDs (565, blue; 605, green; 655, yellow; 705, magenta; 800, red) intracutaneously into the middle digits of the bilateral upper extremities, the bilateral ears, and at the median chin, as shown in the schema. Five primary draining lymph nodes were simultaneously visualized with different colors through the skin. Adapted from Ref. [139]; © 2007, American Chemical Society.

1.4.3.4 *In Vivo* Whole-Body Tumor Imaging in Animals

Although the ability to visualize and identify tumors in living organisms is invaluable for clinical diagnostic applications, the imaging of tumors presents certain challenges, not only from the need for sensitive and specific imaging agents but also from the fundamental barriers to optical imaging in biological tissues. On the other hand, tumor tissues possess certain unique biological attributes that can facilitate optical imaging using nanoparticles such as QDs. During tumor-induced angiogenesis, blood vessels are formed abnormally with erratic architectures and wide endothelial pores. The highly permeable vasculature, in combination with a lack of effective lymphatic drainage, allow large molecules and particulates (up to ~400 nm in size) to extravasate and accumulate in the tumor microenvironment, a phenomenon called the "enhanced permeability and retention" (EPR) effect [180]. The EPR effect has facilitated the use of a variety of nanoparticles, including QDs, for cancer imaging and targeting.

1.4.3.4.1 **QD Conjugates as Active Targeting Probes for Molecular Imaging** Due to the high permeability of tumor vasculature, cancer cells are effectively exposed to the constituents of the bloodstream. Surface antigens on cancerous cells may therefore be used as active targets for molecular imaging using bioaffinity fluorescence probes. *Molecular imaging* is the generation of image contrast due to the molecular differences in tissue (e.g., presence or absence of tumor antigens), rather than to differences in tissue-induced radiation attenuation, as are used in other imaging techniques. Molecular imaging has become an area of tremendous interest in oncology because of its potential to detect early-stage cancers and their metastases. In this respect, QDs have demonstrated great superiority over organic fluorescent dyes for these applications, due to their intense fluorescence signals, long-lasting photostabilities, and unique capabilities for multiplexing, and for enabling the long-term, simultaneous imaging of multiple cancer biomarkers with high degrees of sensitivity and selectivity.

In 2202, Akerman *et al*. first reported the use of QD conjugates for the specific targeting of tumors [60], where QDs attached with tissue-specific peptides were injected intravenously into mice bearing human tumor xenografts. Although the probe detections were not performed in living animals, but rather on embedded tissue specimens, the *in vitro* histological results revealed that the QDs homed to tumor vessel guided by the peptides, and were able to escape clearance by the reticuloendothelial system (RES). It was also shown in this study that the addition of PEG to the QD coating prevented the nonselective accumulation of QDs in the RES.

The first demonstration of targeted molecular imaging using QDs in live animals was made by Gao *et al*. in 2004 [39]. For this, the authors used a new class of multifunctional QD probe for the simultaneous targeting and imaging of subcutaneous human prostate tumors in mice after intravenous injection of QDs conjugated to an antibody against PSMA. The QD conjugate contained an amphiphilic triblock copolymer for *in vivo* protection, and also targeting ligands for tumor antigen recognition and multiple PEG molecules for improved biocompatibility and circulation. Subsequent tissue section microscopy and whole-animal spectral imaging revealed that, whilst QD accumulation in the tumor was primarily due to antibody–antigen binding, it was also aided by the EPR effect. These early studies also introduced the concept of multicolor imaging of QD-tagged cancer cells, opening new possibilities for the ultrasensitive and simultaneous imaging of multiple biomarkers involved in cancer metastasis and invasion. The method used to prepare the QD probe has been published [181]. Similarly, Cai *et al*. used NIR QDs labeled with RGD peptide for the active targeting and imaging of subcutaneous human glioblastoma tumors in mice [133]. Subsequently, Yu *et al*. also achieved active targeting and imaging of human hepatoma in mice with QDs conjugated to an antibody against alpha-fetoprotein (AFP) [141], which is an important biomarker for hepatocellular carcinoma. Very recently, Cheng *et al*. conjugated QDs with DNS and injected the QD probes intravenously into mice bearing CT26/DNS tumors [100]. Subsequent whole-body imaging at 2 h after injection revealed the DNS-QDs to be retained preferentially in the tumor location,

which in turn indicated that the QD conjugates could be used for the targeted imaging of DNS receptor expression *in vivo*.

Tada *et al*. studied the biological processes involved in the active targeting of tumors by QDs [142]. For this, QDs labeled with anti-HER2 monoclonal antibody were used to target human HER2-overexpressing breast cancer in mice. After systemic QD administration, the molecular process was examined in terms of its mechanistic delivery to the tumor by using a high-speed confocal microscope fitted with a high-sensitivity camera. The movement of single QD–antibody complexes could be clearly observed as they circulated in the bloodstream, extravasated into the tumor, diffused into the ECM, bound to their receptors on the tumor cells, and then translocated into the perinuclear region of the cells. The image analysis of the delivery processes of single particles *in vivo* provides valuable information on antibody-conjugated therapeutic nanoparticles, which will undoubtedly be useful for increasing therapeutic efficacies.

Diagaradjane *et al*. reported the first pharmacokinetic and biodistribution study of QD imaging probes for targeted *in vivo* tumor imaging [143]. Here, the NIR QDs were coupled to EGF and injected systemically into mice bearing HCT116 xenograft tumors. *In vivo* imaging showed the EGF-QDs to be mainly distributed in the liver and lymph nodes shortly after injection, and then to accumulate progressively in the tumors, presumably due to a specific binding of the QD–EGF conjugates to EGFR on the tumor cells. The maximum contrast was reached at 4 h after systemic administration. Subsequent immunofluorescence images showed the diffuse colocalization of EGF–QD fluorescence within EGFR-expressing tumor parenchyma, compared to a patchy perivascular sequestration of unconjugated QDs. These results implied that the QD–EGF nanoprobe might permit the quantifiable and repetitive imaging of EGFR expression in tumors. In a similar pharmacokinetic study, Weng *et al*. reported that the systemic administration of liposomes tethered with QDs and an anti-HER2 antibody single-chain F_v fragment resulted in tumor localization and *in vivo* fluorescence imaging in a MCF-7/HER2 xenograft mouse model (Figure 1.11) [107]. These authors found that, although the conjugation of QDs to liposomes increased the average diameter of the labeled liposomal nanoparticles, it effectively eliminated the nonspecific binding observed with QDs alone and enabled an extended circulation time *in vivo*. Chen *et al*. used QDs linked to monoclonal antibody for AFP as a probe for the targeted imaging of human hepatocellular carcinoma xenograft growing in nude mice after injection of the QD probes into a tail vein [125]. On examining the hemodynamics and tissue distribution of the QD probes, they were found to be mainly distributed in the liver and spleen, both of which incorporate the RES. Some QDs were also found in the kidneys, although this may be related to their elimination. Similar findings were later reported by Yang *et al*., who used QDs conjugated with a single-chain anti-EGFR antibody for targeted imaging in nude mice bearing intrapancreatic human xenograft tumors [140].

1.4.3.4.2 **QDs as Nontargeting Contrast Agents for Optical Imaging** In the case where no cellular biomarker is available for the targeted molecular imaging of

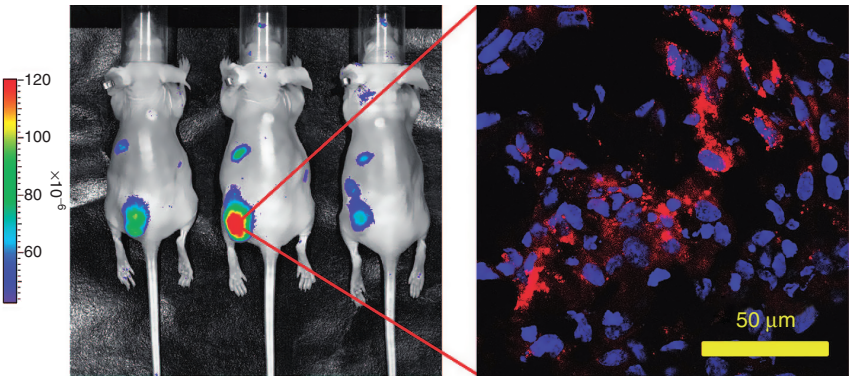

Figure 1.11 *In vivo* targeted fluorescence imaging in a MCF-7/HER2 xenograft mouse model. Left: *In vivo* fluorescence imaging of three nude mice bearing MCF-7/HER2 xenografts implanted in the lower back 30 h after intravenous injection with anti-HER2 QD-ILs. Imaging showed that QD-ILs had localized prominently in tumors, as well as in mononuclear phagocytic system (MPS) organs. Units: efficiency (the fractional ratio of fluorescence emitted per incident photon). Right: A 5 µm section cut from frozen tumor tissues harvested at 48 h post-injection and examined by confocal microscopy using a 63× oil immersion objective (image size, 146 µm × 146 µm). QD-ILs are likely internalized to the cytosol of MCF-7/HER2 cells. From Ref. [107]; © 2008, American Chemical Society.

cancer, nontargeted passive imaging may be attempted. Currently, QDs can be used as powerful imaging contrast agents for studying the complex anatomy and pathophysiology of cancer in animal models.

A solid tumor is composed of cancer and host cells embedded in an ECM and nourished by blood vessels. Whilst a prerequisite to understanding tumor pathophysiology is an ability to distinguish and monitor each component in dynamic studies, standard fluorophores hamper the simultaneous intravital imaging of these components. Stroh *et al.* showed that QDs would greatly enhance current intravital microscopy techniques for the imaging of tumor microenvironment [130], by using QDs as fluorescent contrast agents for blood vessels using two-photon excitation, and concurrently imaging and differentiating tumor vessels from both the perivascular cells and the ECM. The use of QDs allowed a stark contrast to be made between the tumor constituents, due to their intense brightness, tunable wavelengths, and reduced propensity to extravasate into the tumor in comparison with organic dyes. These authors also used QD-tagged beads of varying sizes to model the size-dependent distribution of nanoparticles in tumors.

For nontargeted tumor imaging, it is critical that ways are developed to allow QDs to accumulate at the tumor site. Recent studies on the biodistribution of QDs in living mice have revealed that they are cleared from the circulation primarily by phagocytosis of the nanoparticles by the RES in the liver, spleen, and lymph nodes [182, 183]. The primary phagocytic cells of the RES are monocytes and/or macrophages, including circulating macrophages, perivascular macrophages, and tissue macrophages. Experimental data have suggested that peripheral tissue macro-

phages are capable of phagocytosing QDs, whilst in the brain a macrophage-derived cell – the microglia – is also capable of the phagocytosis of nanoparticles [184]. QDs with surface modifications that improve their blood circulation half-life might escape from the reticuloendothelial cells of the liver, spleen, and lymph nodes, allowing tissue macrophages to phagocytose the circulating QDs. When Muhammad *et al.* used QDs to image tumors in a rat glioma model [144] they found that, after intravenous injection, the QDs were uptaken by macrophages that colocalized within the experimental glioma. In this way, the deposition of QD-laden macrophages within the experimental glioma allowed optical detection of the glioma in the animals. The adaptation of these techniques to the surgical management of gliomas has the potential to reduce the operating time, and to improve not only the diagnostic accuracy but also patient outcomes in glioma therapy.

1.4.4
Multimodality Tumor Imaging

In vivo imaging using QD-based fluorescent probes is limited by the depth of tissue penetration, the lack of anatomic resolution and spatial information, and difficulties in quantitation. In order to overcome these obstacles, the QD surface can be modified (through versatile chemistry) to accommodate multiple imaging (radionuclide or paramagnetic) probes so as to allow for multimodality imaging, by coupling QD-based optical imaging with other imaging modalities such as PET, SPECT, and MRI. One of the most promising applications for QDs is the development of multifunctional QD-based probes for multimodality cancer imaging *in vivo*. A multimodality approach would make it possible to image targeted QDs at all scales, from whole-body down to nanometer resolution, and using a single probe. This would in turn permit elucidation of the targeting mechanisms, biodistribution, and dynamics in living animals with higher sensitivity and/or accuracy.

To allow for quantitative targeted imaging in deep tissues, Chen and colleagues developed a dual-modality imaging probe for both NIR fluorescence imaging and PET, by attaching ^{64}Cu to the polymeric coating of QDs through a covalently bound chelating compound [145]. The targeted *in vivo* imaging of a subcutaneous tumor in mouse, by using this probe, was achieved by simultaneously attaching $\alpha_v\beta_3$ integrin-binding RGD peptides onto the QD surface. The quantification ability and ultrahigh sensitivity of PET imaging enabled the quantitative analysis of the biodistribution and targeting efficacy of this dual-modality imaging probe in glioblastoma-bearing mice. However, the full potential of *in vivo* dual-modality imaging was not realized in this study, as fluorescence was used only as an *ex vivo* imaging tool to validate the *in vivo* results of PET imaging, primarily due to the lower sensitivity of optical imaging in comparison with PET. In a more recent study, the same group constructed a similar QD conjugate and achieved *in vivo* dual PET and NIR fluorescence imaging in the same animal model (Figure 1.12) [146]. This time-targeted imaging of tumor vasculature was achieved by attaching the VEGF protein onto the QD surface so as to specifically target the VEGF receptors

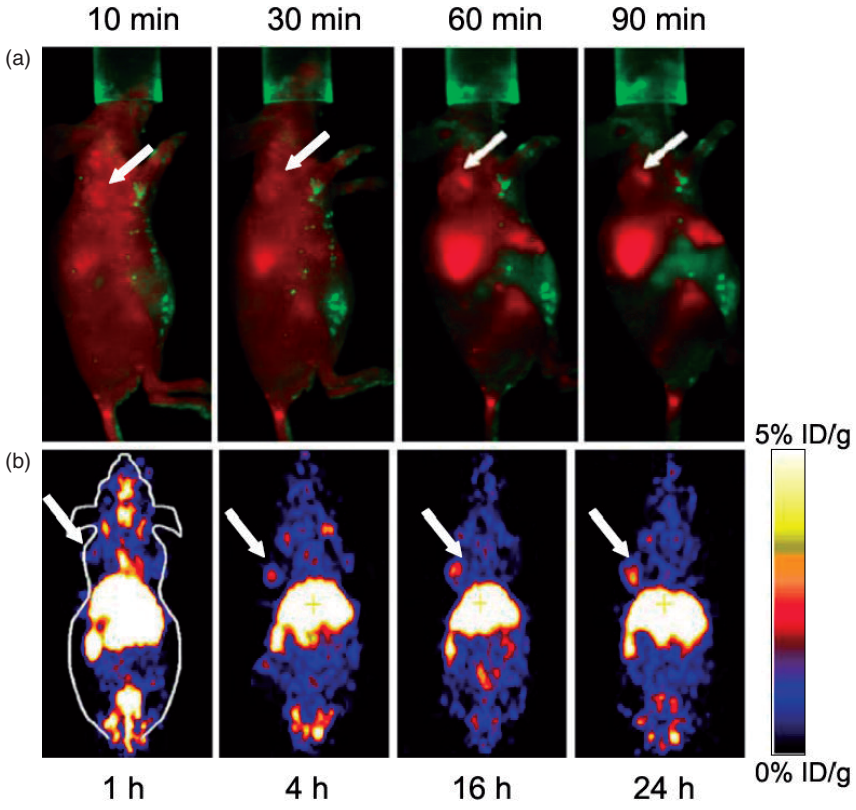

Figure 1.12 Dual modality *in vivo* fluorescence and PET imaging of U87MG tumor-bearing mice. (a) NIR fluorescence imaging at 10, 30, 60, and 90 min post-injection of 200 pmol of DOTA-QD-VEGF; (b) Whole-body coronal PET images at 1, 4, 16, and 24 h post-injection of ca. 300 μCi of ^{64}Cu-DOTA-QD-VEGF. The arrows indicate the tumor. Adapted from Ref. [146]; © 2007, Springer-Verlag.

(VEGFRs) through strong VEGF–VEGFR interaction. VEGFR, which is expressed almost exclusively on the vasculature, serves as a prime target for QD-based imaging, since extravasation is not required to observe the signal. The success of this bifunctional imaging approach may render a higher degree of accuracy for the quantitative targeted NIR fluorescence imaging in deep tissues.

As apoptosis plays an important role in the etiology of a variety of diseases, including cancer, its visualization would allow both an early detection of therapy efficiency and an evaluation of disease progression. To this end, van Tilborg *et al.* developed a dual-modality imaging probe for both optical imaging and MRI by encapsulating QDs in a paramagnetic micelle containing gadolinium [147]. By attaching the nanoparticles with annexin A5, the value of this probe for labeling apoptotic cells *in vitro* could be demonstrated, with a significant T_1 contrast

enhancement with a brightening effect in MRI, as well as an easily detectable fluorescence signal from QDs, being observed. The results of the study suggested a high potential for QD-based dual-modality nanoprobes for the *in vivo* detection of apoptosis with both intravital fluorescence microscopy and MRI.

MRI is preferable for molecular imaging due to its excellent spatial resolution and soft tissue contrast. Although molecular MRI potentially allows the direct covisualization of tumor angiogenic activity with anatomy, its inherently low sensitivity may be problematic due to the typically low abundance of upregulated biomolecules. However, this difficulty can be overcome by using large-molecular-weight constructs capable of carrying a high payload of paramagnetic dopants, and multiple targeting ligands to enhance the relaxivity and targeting efficacy, respectively, of the MRI probe. Oostendorp *et al*. developed a new class of paramagnetic QDs (pQDs) by attaching biotin-poly(lysine) dendritic gadolinium to the surface of streptavidin-bound QDs. The probe was labeled with cyclic Asn-Gly-Arg (cNGR) for the noninvasive assessment of tumor angiogenic activity, using quantitative *in vivo* MRI [148]. cNGR colocalizes with an aminopeptidase (CD13) that is highly overexpressed on the angiogenic tumor endothelium. An intravenous injection of cNGR–pQDs in tumor-bearing mice resulted in an increased quantitative contrast, allowing *in vivo* quantification and accurate localization of angiogenic activity (Figure 1.13). Since, similar to the previously mentioned PET study [145], QD fluorescence was used only *ex vivo*, and not *in vivo*, the full potential of *in vivo* dual-modality imaging was not realized in this study.

1.4.5
Dual-Functionality QDs for Cancer Imaging and Therapy

Drug-laden nanoparticles have shown great promise for targeted drug delivery into tumors. A premise of nanomedicine is that it may be feasible to develop multifunctional constructs that combine diagnostic and therapeutic capabilities, thus leading to a better targeting of drugs to diseased cells. The large surface area of QDs, combined with their versatile surface chemistry, makes them convenient scaffolds to accommodate anticancer drugs, either through chemical linkage or by simple physical immobilization, leading in turn to the development of nanostructures with integrated imaging and therapy functionalities. Bagalkot *et al*. reported a multifunctional system which comprised a QD, RNA aptamers, and the anticancer drug doxorubicin (Dox) for targeted cancer imaging, drug delivery, and sensing [149]. The RNA aptamers were attached covalently to the surface of the QDs to serve as targeting molecules for the extracellular domain of PSMA. The intercalation of Dox in the double-stranded stem of the aptamer resulted in a targeted tertiary conjugate with reversible self-quenching properties based on a bi-FRET (fluorescence resonance energy transfer) mechanism, one between QD and Dox and another between Dox and the aptamer. As demonstrated in the *in vitro* experiment, the multifunctional nanoparticle system can first deliver Dox to the targeted prostate cancer cells, and then sense the release of Dox by activating the fluorescence of QD, which concurrently images the cancer cells. By

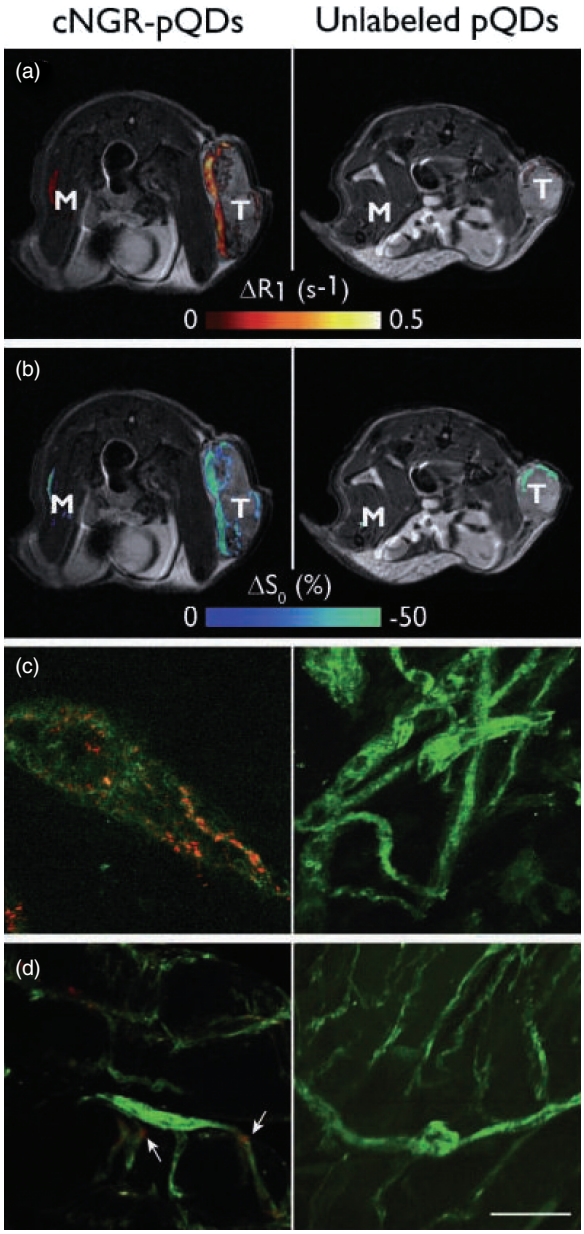
cNGR-pQDs
Unlabeled pQDs
(a)
M
T
M
T
ΔR1 (s-1)
0
0.5
(b)
M
T
M
T
ΔS0 (%)
0
-50
(c)
(d)

Figure 1.13 T_2-weighted anatomic MRI images with color overlay of ΔR_1 (a) and ΔS_0 (b) for tumor (*T*) and muscle (*M*) tissue of mice injected with cNGR-labeled or unlabeled pQDs ($n = 7$ for both groups). Changes in R_1 were most pronounced at the tumor rim for cNGR-pQDs. Although an R_1 increase in the tumor rim was also observed for unlabeled pQDs, the average response was threefold lower when compared to cNGR-pQDs, indicating a high specificity of cNGR for angiogenic tumor endothelium. This is further supported by the low changes in R_1 found in muscle tissue. Changes in S_0 (b) colocalized almost completely with changes in R_1 (a). Representative TPLSM images of tumor (c) and muscle tissue (d) showing pQD signal (red) and EC-specific αCD31-FITC (green). The cNGR-pQDs accurately colocalized with tumor ECs, indicating binding of the contrast agent to the tumor endothelium (c). The cNGR-pQDs were also detected in muscle tissue with TPLSM (arrows in d), although to a much lesser extent than in tumor tissue. The cNGR-pQDs did not display any colocalization with muscle ECs, and were only found intraluminally. Unlabeled pQDs were not or only sparsely detected in both tumor and muscle tissue. Scale bar = 50 μm. From Ref. [148]; © 2008, American Association for Cancer Research.

incorporating multiple CG sequences within the stem of the aptamers, the drug-loading capacity of the system can be further increased, thereby enhancing the therapeutic efficacy of the conjugates. While this study was at a proof-of-concept stage, using only cultured cancer cells, a subsequent study by Weng *et al.* proved to be more immediately relevant to the *in vivo* imaging and treatment of solid tumors [107]. Here, a multifunctional QD-conjugated immunoliposome system (QD–ILs) was developed for tumor-cell targeting, imaging, and drug delivery, where anti-HER2 single chain Fv fragments were attached to the surface of the nanoparticle for targeted delivery to HER2-expressing breast cancer cells. The anticancer drug Dox was encapsulated in the aqueous interior of the liposome (Figure 1.14). *In vitro* experiments indicated that Dox-loaded QD–ILs were internalized by HER2-expressing cancer cells through receptor-mediated endocytosis, and showed an efficient anticancer activity. In MCF-7/HER2 xenograft mouse models, the localization of QD-ILs at tumor sites was confirmed by *in vivo* fluorescence imaging (see Figure 1.11). It was also shown that QD–ILs could significantly prolong the circulation of QDs in the bloodstream. Although the anticancer activity of the Dox-loaded QD–ILs was not demonstrated *in vivo*, these studies will nonetheless guide the future design and optimization of multifunctional nanoparticle agents for *in vivo*-targeted tumor imaging and therapy.

Recently, RNA interference (RNAi) has become a powerful technology for sequence-specific gene suppression. Although RNAi-effectuated oncogene silencing using siRNA represents an effective means of targeted gene therapy for various cancers [185], the application of RNAi *in vivo* has been hampered by its rapid excretion and nontargeted tissue distribution during systemic delivery. In order to develop and optimize methods for the efficient delivery of siRNA into tumor cells, QDs may also provide a versatile nanoscale scaffold to develop multifunctional nanoparticles for targeted siRNA delivery and imaging of the delivery process. In this regard, Derfus *et al.* used QDs as a scaffold to conjugate siRNA against enhanced green fluorescent protein (EGFP) and tumor-homing peptide F3

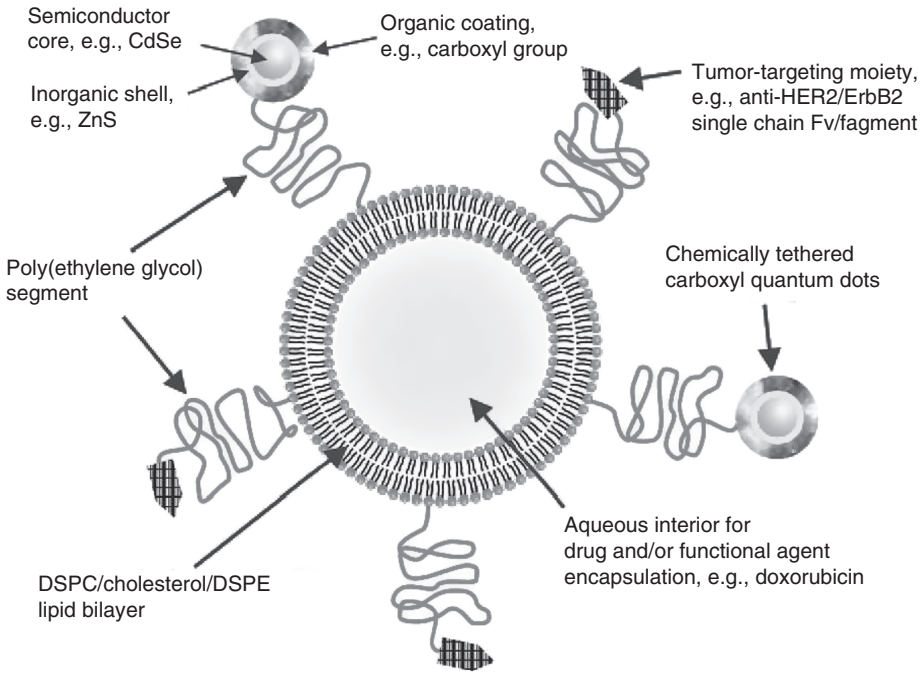

Figure 1.14 Schematic showing the structure of a QD–IL nanoparticle. The liposomal core is about 100 nm in diameter, as visualized by freeze-fracture electron microscopy (ff-EM). Derivatized CdSe/ZnS core–shell QDs are represented as a sphere with a layer of organic coating (gray) covering the outer surface of the inorganic shell (yellow) and the semiconductor core (orange). They were also characterized by ff-EM, indicating an average diameter of ~11 nm. Surface-derivatized QDs were chemically linked to functionalized PEG-DSPE incorporated in extruded liposomes. Anti-HER2 single chain Fv fragments (scFv, arrowheads) are attached to the end of PEG chains. scFv moieties (MW ~ 25 kDa) are not drawn to scale. The QD–ILs retain an aqueous interior for loading and delivery of drugs/probes. From Ref. [107]; © 2008, American Chemical Society.

to functional groups on the QD surface. The F3 peptide, targeting cell-surface nucleolin, was attached to achieve targeted internalization by tumor cells. It was shown that the delivery of these F3/siRNA–QDs to EGFP-transfected HeLa cells, and release from their endosomal entrapment, led to a significant knockdown of the EGFP signal [150]. Although this study was only a proof-of-concept, by designing the siRNA sequences against oncogenes instead of EGFP, this technology might ultimately be adapted for the simultaneous imaging and treatment of cancers. More recently, Yezhelyev *et al.* reported a multifunctional nanoparticle system for siRNA delivery and imaging using QDs with proton-absorbing polymeric coatings ("proton sponges") [128]. By optimizing the proton-absorbing capacity through balancing the composition of the tertiary amine and carboxylic acid groups on the QD surface, an endosomal release of the siRNA was achieved via the proton sponge effect. As a result, a dramatic (10–20-fold) improvement in gene silencing efficiency, and a simultaneous five- to sixfold reduction in cellular

toxicity, compared to existing transfection agents, was observed in MDA-MB-231 cells. The QD–siRNA nanoparticles were also dual-modality optical and electron-microscopy probes, allowing real-time tracking and the ultrastructural localization of QDs during delivery and transfection. These new insights and capabilities represent a major step towards nanoparticle engineering for combined imaging and therapeutic applications.

1.5
Quantum Dot Cytotoxicity and Potential Safety Concerns

One major obstacle to fully exploring the *in vivo* applications of QDs in biomedical imaging is the concern regarding their possible cytotoxicity. Compared to gold and iron oxide nanoparticles (which have been used for several decades and have proved to be biocompatible), QDs are relatively new materials and their toxicity has not yet been fully characterized. Prior to any clinical applications on human subjects, the biocompatibility of QDs must be characterized and any potential safety concerns clarified.

A detailed discussion on the topic of QD toxicity may warrant a separate chapter, or even a book. In addition, a number of dedicated reviews have been published that summarize much of what is known in this area. Hoet *et al.* reviewed most of the data available up to 2004 on the health effects of nanoparticles in general [186], and some later reviews have since updated the topic, with data extended to 2007 [6, 187]. In 2006, Hardman published one of the most extensive reviews on the toxicity of QDs in particular, in which the cumulative results from almost all previous *in vivo* studies (both cellular and small animal) were summarized [188]. Therefore, only a brief outline of previous major findings will be provided here, and some of the most recent studies highlighted.

One source of QD cytotoxicity derives from the semiconductor materials that are commonly found in the QD core, such as the heavy metals Cd and Se, the toxicities of which are well known. Under certain circumstances, these elements may leach from the QDs. By using hepatocytes, Derfus *et al.* showed that the oxidation of Cd on the QD surface and subsequent Cd^{2+} release, mediated by oxygen or ultraviolet light, is one possible mechanism responsible for QD cytotoxicity [189]. The protective shell, which in most cases is ZnS, has a much lower toxicity than the core; thus, adding a protective shell may result in a significant reduction in the cytotoxic effects of QDs, as well as improving their optical properties [189, 190]. Most current studies have indicated that, when properly capped by both ZnS and hydrophilic shells, no acute and obvious QD-induced toxicity was detected in studies of cell proliferation and viability or systemic toxicity in mice [191]. For example, *in vivo* studies performed by Ballou *et al.* indicated that stably protected QDs had no apparent toxicity in mice over long periods of time [192]. However, the introduction of capping layers may still be insufficient to solve the problem of cytotoxicity completely, as various other factors, including the aggregation of particles on the cell surface [51] and even the stabilizing QD surface ligands

[193], have been shown to impair cell viability. Hence, the choice of an appropriate surface coating has also been shown to be a critical parameter, since simple coatings (e.g., thiol-containing carboxylic acids) present only a minor diffusion barrier for Cd^{2+}. Thiol-coated QDs are also known for their poor colloidal stability [194, 195]; consequently, the introduction of inert and stable, macromolecular or crosslinked surface coatings, may be an important improvement [196].

QD cytotoxicity should not be attributed solely to the toxic effect of Cd^{2+} released from the particle core [197]. Another source of QD toxicity derives from the reactive oxygen species (ROS) generated during excitation [197–200], since QDs can transfer absorbed optical energy to oxygen molecules. Free radicals can cause damage to DNA [201] and other cellular components and, as a consequence, induce apoptosis and necrosis.

It should be pointed out that the unique structure of QDs presents a complex set of physico-chemical characteristics that compounds studies in this area. The QD cores can be constituted from different combinations of binary semiconductors such as CdSe, CdTe, CdS, and InP. Further, the cores are commonly encapsulated with a protective layer and are then functionalized with a variety of surface-coating ligands that include small thiolated molecules or larger amphiphilic polymers for aqueous compatibility. In fact, surface coatings have been found to be determinants of QD cytotoxicity [112, 202, 203]. Additionally, the QDs may exist in a wide range of sizes, with diameters ranging from a few nanometers to more than 10 nm, which may also affect their cytotoxicity [112]. For biological use, QDs can be further modified with various proteins or nucleic acids. Cumulatively, this combination of materials and physical properties serves to confound any systematic study of toxicity, even before issues such as dosage or exposure time are formally addressed. As a result, most of the studies in the past have primarily been observational in nature, where authors have reported the effects of a given QD material on a particular cell line or animal, at some specified concentration(s) for some exposure time [186–188]. Consequently, the results were mixed with some which reported no visible toxicity [123, 204], while others reported high cytotoxicity [205]. This can be interpreted to reflect what is posited above: the choice of core–shell material and solubilization cap, in conjunction with the dosage/exposure time, will obscure any simple assessments of toxicity. Therefore, more systematic and extensive studies are required in order to fully understand the toxicity of QDs. Recently, Chen *et al.* conducted a systematic study of the effect of dosage on cytotoxicity using a QD–antibody conjugate [125]. The results from this *in vitro* study on the human hepatocellular carcinoma cell line HCCLM6 indicated that the QD cytotoxicity was dose-dependent. For example, with a dose of $1 \times 10^7\,\mathrm{mol\,l^{-1}}$ or less, there were no discernable adverse effects on cell growth and development, but when the dose exceeded $1 \times 10^7\,\mathrm{mol\,l^{-1}}$ a significant decrease in cell viability was observed. *In vivo* studies with nude mice at a dose of $1 \times 10^5\,\mathrm{mol\,l^{-1}}$ showed no evidence of acute toxicity in the test group as compared to the control groups.

Besides cytotoxicity, another concern over QD safety for clinical applications is their degradation, metabolism, and body clearance, which has not been studied until recently. When Fischer *et al.* [206] investigated the distribution, sequestration, and clearance of mercaptoundecanoic acid-functionalized QDs in rats, the

QDs coated with BSA were shown to be cleared more rapidly from serum than those coated with crosslinked lysine. Further, almost all (99%) of the BSA-coated QDs were found in the liver after 90 min, as compared to only 40% of the lysine QDs. These results may reflect one of the primary metabolic roles of endogenous serum albumin. Interestingly, these QDs were not excreted by rats, even after 10 days. Recent studies on the biodistribution of QDs in live mice have revealed that QDs can accumulate in the liver, spleen, and lymph nodes for significant periods of time after systemic injection [107, 125, 140, 143, 182, 183].

Since QDs contains toxic materials, an understanding of the toxicity mechanisms and the process of clearing nanoparticles from animal and human bodies should be given serious attention in the near future. Recent studies have indicated that even though QDs did not affect cell morphology, they might alter the expression of specific genes [207, 208], and therefore the potential risk at the molecular level and the long-term effects of QDs on humans and the environment should be carefully and extensively evaluated. However, there is at present a general paucity of information on molecular mechanistic studies of QD toxicity. When Choi *et al.* examined the cytotoxicity of QDs in human neuroblastoma cells, they found that CdTe QD-induced toxicity was correlated with Fas upregulation on the surface of treated cells and an increased membrane lipid peroxidation, that may lead to an impaired mitochondrial function (Figure 1.15) [209]. It was also found that QDs modified by *N*-acetylcysteine (NAC), an antioxidant, were internalized to a lesser extent by the cells and were less cytotoxic than unmodified QDs.

Currently, several strategies have been developed to overcome the potential toxicity of QDs. More stable and robust coatings can be developed to protect the QD surfaces from oxidative environments, and QDs may also be encapsulated inside polymeric nanoparticles for further protection. For example, Pan and Feng used nanoparticles composed of a mixture of two vitamin E-containing copolymers to encapsulate QDs in order to reduce their side effects, as well as to improve their imaging effects. Compared to the free QDs, the QDs formulated in polymeric nanoparticles showed a lower *in vitro* cytotoxicity for both MCF-7 cells and NIH-3T3 cells [151]. In addition, more effective targeting systems can be employed to increase the detection efficiency and reduce the required dose of QDs [200]. Another possible strategy might be to develop new, high-quality QD systems that do not contain potentially biologic toxic components. For example, Pradhan *et al.* have synthesized Cu- or Mn-doped ZnSe QDs with acceptable quantum efficiency and optical properties [190]. Clearly, progress made using these new strategies will ultimately lead to improved cytotoxicity profiles for QDs.

1.6
Concluding Remarks and Future Perspectives

QDs, as a novel class of fluorescent probes, have lived up to many of their promises for the molecular imaging of cancers. With rapid advances in their synthesis, surface modification and bioconjugation, significant progress has been made in applying QDs to potentially useful clinical applications, such as profiling cancer

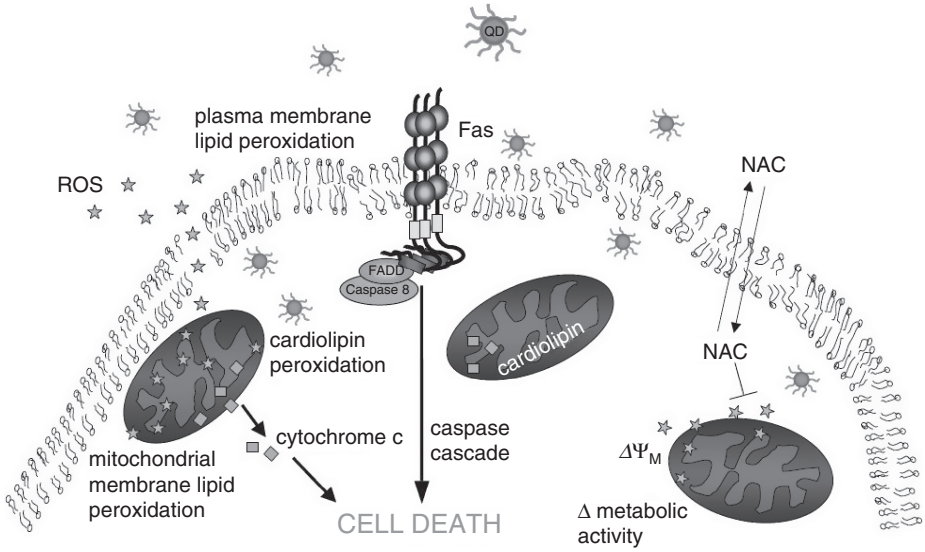

Figure 1.15 Proposed mechanism of QD-induced cell death involving Fas, lipid peroxidation, and mitochondrial impairment. Cells exposed to cadmium telluride QDs (unmodified and NAC-modified) induce ROS which causes Fas upregulation and plasma membrane lipid peroxidation. Apoptotic cell death is induced by activation of Fas and its downstream effectors. Lipid peroxidation also occurs at the mitochondrial membranes, degrading cardiolipin, changing the mitochondrial membrane potential, eventually leading to the release of cytochrome c, and promoting apoptotic cascades. NAC bound to the QD surface, modifies the extent of QD internalization, which is correlated with cell death, upregulation of Fas, and ROS induced lipid peroxidation. NAC treatment (2–5 mM) abolishes oxidative stress, induces antioxidant enzymes, and attenuates mitochondrial impairment. From Ref. [209]; © 2007 Choi *et al.*).

biomarkers in pathologic specimens, the *in vivo* imaging of cancer and metastasis, and monitoring the clinical responses of tumors to therapy. In addition, the potential for using QDs in multimodality imaging and for combined imaging and therapy has also been demonstrated. Despite all of these successes, several challenges remain for enhancing sensitivity, maximizing specificity, and minimizing toxicity, all of which are areas to which future research should be directed. In particular, the question of intrinsic toxicity and long retention times of the QD probes within the body represent significant challenges to their medical use, and these problems must be solved before clinical applications can proceed. Nonetheless, this exciting new technology holds great promise for improving the diagnosis and treatment of patients with cancers.

Abbreviations

ACTH	adrenocorticotropic hormone
AFP	alpha-fetoprotein

BSA	bovine serum albumin
CA	cancer antigen
CAM	cell adhesion molecule
CD	cluster of differentiation
CEA	carcinoembryonic antigen
cNGR	cyclic asparagine-glycine-arginine
CT	computed tomography
DAPI	4′,6-diamidino-2-phenylindole
DNA	deoxyribonucleic acid
DOTA	1,4,7,10-tetraazacyclododecane-1,4,7,10-tetraacetic acid
Dox	doxorubicin
EGF	epidermal growth factor
EGFP	enhanced green fluorescent protein (GFP)
EGFR	epidermal growth factor receptor
EPR	enhanced permeability and retention
ER	estrogen receptor
ff-EM	freeze-fracture electron microscopy
FFPE	formalin-fixed and paraffin-embedded
FISH	fluorescence *in situ* hybridization
FITC	fluorescein isothiocyanate
FRET	fluorescence resonance energy transfer
GFP	green fluorescent protein
HER	human epidermal growth factor receptor
HER2	human epidermal growth factor receptor 2
HSP	heat-shock protein
IHC	immunohistochemistry
IL	immunoliposome
*iso*DGR	isoaspartate-glycine-arginine
LSC	laser scanning cytometry
MB	molecular beacon
MMP	matrix metalloprotease
MPS	mononuclear phagocytic system
MRI	magnetic resonance imaging
mRNA	messenger ribonucleic acid (RNA)
NAC	*N*-acetylcysteine
NFS	National Science Foundation
NIH	National Institutes of Health
NIR	near-infrared
PEG	polyethylene glycol
PEG-DSPE	*N*-(polyethylene glycol)-1,2-distearoyl-*sn*-glycero-3-phosphoethanolamine
PET	positron emission tomography
pQD	paramagnetic quantum dot (QD)
PSA	prostate-specific antigen
PSMA	prostate-specific membrane antigen

QD	quantum dot
RES	reticuloendothelial system
RGD	arginine-glycine-aspartate
RNA	ribonucleic acid
RNAi	RNA interference
ROS	reactive oxygen species
SCC	squamous cell carcinoma
siRNA	small interfering RNA
SLN	sentinel lymph node
SPECT	single photon emission computed tomography (CT)
THG	third harmonic generation
TMA	tissue microarray
TOPO	trioctylphosphine oxide
TPLSM	two-photon laser scanning microscopy
VEGF	vascular endothelial growth factor
VEGFR	vascular endothelial growth factor (VEGF) receptor

Acknowledgments

Certain commercial equipment or materials have been identified in this chapter in order to specify adequately the experimental procedures. Such identification does not imply recommendation or endorsement by the National Institute of Standards and Technology, nor does it imply that the materials or equipment identified are necessarily the best available for the purpose.

References

1 Freitas, R.A. Jr (2005) What is nanomedicine? *Nanomedicine*, **1**, 2–9.
2 Editorial (2003) Nanomedicine: grounds for optimism, and a call for papers. *Lancet*, **362**, 673.
3 The National Science Foundation (NSF) (2004) NSF Priority Areas, http://www.nsf.gov/od/lpa/news/publicat/nsf04009/cross/priority.htm (accessed 31 March 2009).
4 The National Institutes of Health (NIH) (2009) NIH roadmap for medical research: Nanomedicine – Overview, http://nihroadmap.nih.gov/nanomedicine/ (accessed 31 March 2009).
5 The National Cancer Institute (NCI) (2004) Cancer nanotechnology plan, http://nano.cancer.gov/about_alliance/cancer_nanotechnology_plan.asp (accessed 31 March 2009).
6 Buzea, C., Pacheco, I.I. and Robbie, K. (2007) Nanomaterials and nanoparticles: sources and toxicity. *Biointerphases*, **2**, MR17–71.
7 Efros, Al L. and Efros, A.L. (1982) Interband absorption of light in a semiconductor sphere. *Soviet Physics: Semiconductors*, **16**, 772–5.
8 Ekimov, A.I. and Onushchenko, A.A. (1982) Quantum size effect in the optical-spectra of semiconductor micro-crystals. *Soviet Physics: Semiconductors*, **16**, 775–8.
9 Bruchez, M. Jr, Moronne, M., Gin, P., Weiss, S. and Alivisatos, A.P. (1998) Semiconductor nanocrystals as fluorescent biological labels. *Science*, **281**, 2013–16.

10 Chan, W.C. and Nie, S. (1998) Quantum dot bioconjugates for ultrasensitive nonisotopic detection. *Science*, **281**, 2016–18.

11 Medintz, I.L., Mattoussi, H. and Clapp, A.R. (2008) Potential clinical applications of quantum dots. *International Journal of Nanomedicine*, **3**, 151–67.

12 Tannock, I.F., Hill, R.P., Bristow, R.G. and Harrington, L. (eds) (2005) *The Basic Science of Oncology*, 4th edn, McGraw-Hill Professional, New York.

13 Alberts, B., Bray, D., Lewis, J., Raff, M., Roberts, K. and Watson, J.D. (eds) (1994) *Molecular Biology of the Cell*, 3rd edn, Garland Publishing, New York.

14 Schuiz, W.A. (2005) *Molecular Biology of Human Cancers: An Advanced Student's Textbook*, Springer, New York, pp. 11–17.

15 American Cancer Society (2008) Cancer Facts & Figures 2008, http://www.cancer.org/downloads/STT/2008CAFFfinalsecured.pdf (accessed 31 March 2009).

16 Frangioni, J.V. (2008) New technologies for human cancer imaging. *Journal of Clinical Oncology*, **26**, 4012–21.

17 Debbage, P. and Jaschke, W. (2008) Molecular imaging with nanoparticles: giant roles for dwarf actors. *Histochemistry and Cell Biology*, **130**, 845–75.

18 Chatterjee, S.K. and Zetter, B.R. (2005) Cancer biomarkers: knowing the present and predicting the future. *Future Oncology*, **1**, 35–50.

19 Stamey, T.A., Yang, N., Hay, A.R., McNeal, J.E., Freiha, F.S. and Redwine, E. (1987) Prostate-specific antigen as a serum marker for adenocarcinoma of the prostate. *The New England Journal of Medicine*, **317**, 909–16.

20 Devine, P.L., McGuckin, M.A. and Ward, B.G. (1992) Circulating mucins as tumor markers in ovarian cancer. *Anticancer Research*, **12**, 709–17.

21 Maruvada, P., Wang, W., Wagner, P.D. and Srivastava, S. (2005) Biomarkers in molecular medicine: cancer detection and diagnosis. *Biotechniques*, **38**, S9–15.

22 Duffy, M.J. and Crown, J. (2008) A personalized approach to cancer treatment: how biomarkers can help. *Clinical Chemistry*, **54**, 1770–9.

23 Goldstein, A.N., Echer, C.M. and Alivisatos, A.P. (1992) Melting in semiconductor nanocrystals. *Science*, **256**, 1425–7.

24 Alivisatos, A.P. (1996) Semiconductor clusters, nanocrystals, and quantum dots. *Science*, **271**, 933–7.

25 Sapra, S. and Sarma, D.D. (2004) Evolution of the electronic structure with size in II-IV semiconductor nanocrystals. *Physical Review B*, **69**, 125304.

26 Qu, L. and Peng, X. (2002) Control of photoluminescence properties of CdSe nanocrystals in growth. *Journal of the American Chemical Society*, **124**, 2049–55.

27 Zhong, X., Han, M., Dong, Z., White, T.J. and Knoll, W. (2003) Composition-tunable $Zn_xCd_{1-x}Se$ nanocrystals with high luminescence and stability. *Journal of the American Chemical Society*, **125**, 8589–94.

28 Kim, S., Fisher, B., Eisler, H.-J. and Bawendi, M. (2003) Type II quantum dots: CdTe/CdSe(core/shell) and CdSe/ZnTe(core/shell) heterostructures. *Journal of the American Chemical Society*, **125**, 11466–7.

29 Zhong, X., Feng, Y., Knoll, W. and Han, M. (2003) Alloyed $Zn_xCd_{1-x}S$ nanocrystals with highly narrow luminescence spectral width. *Journal of the American Chemical Society*, **125**, 13559–63.

30 Pietryga, J.M., Schaller, R.D., Werder, D., Stewart, M.H., Klimov, V.I. and Hollingsworth, J.A. (2004) Pushing the band gap envelope: mid-infrared emitting colloidal PbSe quantum dots. *Journal of the American Chemical Society*, **126**, 11752–3.

31 Michalet, X., Pinaud, F.F., Bentolila, L.A., Tsay, J.M., Doose, S., Li, J.J., Sundaresan, G., Wu, A.M., Gambhir, S.S. and Weiss, S. (2005) Quantum dots for live cells, *in vivo* imaging, and diagnostics. *Science*, **307**, 538–44.

32 Efros, A.L. and Rosen, M. (2000) The electronic structure of semiconductor nanocrystals. *Annual Review of Materials Science*, **30**, 475–521.

33 Leatherdale, C.A., Woo, W.-K., Mikulec, F.V. and Bawendi, M.G. (2002) On the absorption cross section of CdSe nanocrystal quantum dots. *The Journal of Physical Chemistry B*, **106**, 7619–22.

34 Dabbousi, B.O., Rodriguez-Viejo, J., Mikulec, F.V., Heine, J.R., Mattoussi, H., Ober, R., Jensen, K.F. and Bawendi, M.G. (1997) (CdSe)ZnS core-shell quantum dots: synthesis and characterization of a size series of highly luminescent nanocrystallites. *The Journal of Physical Chemistry B*, **101**, 9463–75.

35 Gao, X., Yang, L., Petros, J.A., Marshall, F.F., Simons, J.W. and Nie, S. (2005) *In vivo* molecular and cellular imaging with quantum dots. *Current Opinion in Biotechnology*, **16**, 63–72.

36 Dahan, M., Laurence, T., Pinaud, F., Chemla, D.S., Alivisatos, A.P., Sauer, M. and Weiss, S. (2001) Time-gated biological imaging by use of colloidal quantum dots. *Optics Letters*, **26**, 825–7.

37 Pepperkok, R., Squire, A., Geley, S. and Bastiaens, P.I. (1999) Simultaneous detection of multiple green fluorescent proteins in live cells by fluorescence lifetime imaging microscopy. *Current Biology*, **9**, 269–72.

38 Jakobs, S., Subramaniam, V., Schönle, A., Jovin, T.M. and Hell, S.W. (2000) EFGP and DsRed expressing cultures of *Escherichia coli* imaged by confocal, two-photon and fluorescence lifetime microscopy. *FEBS Letters*, **479**, 131–5.

39 Gao, X., Cui, Y., Levenson, R.M., Chung, L.W. and Nie, S. (2004) *In vivo* cancer targeting and imaging with semiconductor quantum dots. *Nature Biotechnology*, **22**, 969–76.

40 Kortan, A.R., Hull, R., Opila, R.L., Bawendi, M.G., Steigerwald, M.L., Carroll, P.J. and Brus, L.E. (1990) Nucleation and growth of CdSe on ZnS quantum crystallite seeds, and vice versa, in inverse micelle media. *Journal of the American Chemical Society*, **112**, 1327–32.

41 Murray, C.B., Norris, D.J. and Bawendi, M.G. (1993) Synthesis and characterization of nearly monodisperse CdE (E = S, Se, Te) semiconductor nanocrystallites. *Journal of the American Chemical Society*, **115**, 8706–15.

42 Talapin, D.V., Rogach, A.L., Komowski, A., Haase, M. and Weller, H. (2001) Highly luminescent monodisperse CdSe and CdSe/ZnS nanocrystals synthesized in a hexadecylamine–trioctylphosphine oxide–trioctylphospine mixture. *Nano Letters*, **1**, 207–11.

43 Yang, H. and Holloway, P.H. (2004) Efficient and photostable ZnS-passivated CdS:Mn luminescent nanocrystals. *Advanced Functional Materials*, **14**, 152–6.

44 Hines, M.A. and Guyot-Sionnest, P. (1996) Synthesis and characterization of strongly luminescing ZnS-capped CdSe nanocrystals. *The Journal of Physical Chemistry*, **100**, 468–71.

45 Nirmal, M. and Brus, L. (1999) Luminescence photophysics in semiconductor nanocrystals. *Accounts of Chemical Research*, **32**, 407–14.

46 Peng, X., Schlamp, M.C., Kadavanich, A.V. and Alivisatos, A.P. (1997) Epitaxial growth of highly luminescent CdSe/CdS core/shell nanocrystals with photostability and electronic accessibility. *Journal of the American Chemical Society*, **119**, 7019–29.

47 Reiss, P., Bleuse, J. and Pron, A. (2002) Highly luminescent CdSe/ZnSe core/shell nanocrystals of low size dispersion. *Nano Letters*, **2**, 781–4.

48 Gao, X. and Dave, S.R. (2007) Quantum dots for cancer molecular imaging. *Advances in Experimental Medicine and Biology*, **620**, 57–73.

49 Wu, X., Liu, H., Liu, J., Haley, K.N., Treadway, J.A., Larson, J.P., Ge, N., Peale, F. and Bruchez, M.P. (2003) Immunofluorescent labeling of cancer marker Her2 and other cellular targets with semiconductor quantum dots. *Nature Biotechnology*, **21**, 41–6.

50 Dubertret, B., Skourides, P., Norris, D.J., Noireaux, V., Brivanlou, A.H. and Libchaber, A. (2002) *In vivo* imaging of quantum dots encapsulated in phospholipid micelles. *Science*, **298**, 1759–62.

51 Kirchner, C., Liedl, T., Kudera, S., Pellegrino, T., Javier, A.M., Gaub, H.E., Stölzle, S., Fertig, N. and Parak, W.J. (2005) Cytotoxicity of colloidal CdSe and CdSe/ZnS nanoparticles. *Nano Letters*, **5**, 331–8.

52 Hild, W.A., Breunig, M. and Goepferich, A. (2008) Quantum dots–nano-sized probes for the exploration of cellular and intracellular targeting. *European Journal*

of Pharmaceutics and Biopharmaceutics, **68**, 153–68.

53 Goldman, E.R., Balighian, E.D., Mattoussi, H., Kuno, M.K., Mauro, J.M., Tran, P.T. and Anderson, G.P. (2002) Avidin: a natural bridge for quantum dot-antibody conjugates. *Journal of the American Chemical Society*, **124**, 6378–82.

54 Lidke, D.S., Nagy, P., Heintzmann, R., Arndt-Jovin, D.J., Post, J.N., Grecco, H.E., Jares-Erijman, E.A. and Jovin, T.M. (2004) Quantum dot ligands provide new insights into erbB/HER receptor-mediated signal transduction. *Nature Biotechnology*, **22**, 198–203.

55 Dahan, M., Lévi, S., Luccardini, C., Rostaing, P., Riveau, B. and Triller, A. (2003) Diffusion dynamics of glycine receptors revealed by single-quantum dot tracking. *Science*, **302**, 442–5.

56 Jaiswal, J.K., Mattoussi, H., Mauro, J.M. and Simon, S.M. (2003) Long-term multiple color imaging of live cells using quantum dot bioconjugates. *Nature Biotechnology*, **21**, 47–51.

57 Zhang, C., Ma, H., Ding, Y., Jin, L., Chen, D. and Nie, S. (2000) Quantum dot labeled trichosanthin. *Analyst*, **125**, 1029–31.

58 Srinivasan, C., Lee, J., Papadimitrakopoulos, F., Silbart, L.K., Zhao, M. and Burgess, D.J. (2006) Labeling and intracellular tracking of functionally active plasmid DNA with semiconductor quantum dots. *Molecular Therapy*, **14**, 192–201.

59 Parak, W.J., Gerion, D., Zanchet, D., Woerz, A.S., Pellegrino, T., Micheel, C., Williams, S.C., Seitz, M., Bruehl, R.E., Bryant, Z., Bustamante, C., Bertozzi, C.R. and Alivisatos, A.P. (2002) Conjugation of DNA to silanized colloidal semiconductor nanocrystalline quantum dots. *Chemistry of Materials*, **14**, 2113–19.

60 Akerman, M.E., Chan, W.C., Laakkonen, P., Bhatia, S.N. and Ruoslahti, E. (2002) Nanocrystal targeting *in vivo*. *Proceedings of the National Academy of Sciences of the United States of America*, **99**, 12617–21.

61 Mattoussi, H., Mauro, J.M., Goldman, E.R., Anderson, G.P., Sundar, V.C., Mikulec, F.V. and Bawendi, M.G. (2000) Self-assembly of CdSe-ZnS quantum dot bioconjugates using an engineered recombinant protein. *Journal of the American Chemical Society*, **122**, 12142–50.

62 Hanaki, K.I., Momo, A., Oku, T., Komoto, A., Maenosono, S., Yamaguchi, Y. and Yamamoto, K. (2003) Semiconductor quantum dot/albumin complex is a long-life and highly photostable endosome marker. *Biochemical and Biophysical Research Communications*, **302**, 496–501.

63 Goldman, E.R., Anderson, G.P., Tran, P.T., Mattoussi, H., Charles, P.T. and Mauro, J.M. (2002) Conjugation of luminescent quantum dots with antibodies using an engineered adaptor protein to provide new reagents for fluoroimmunoassays. *Analytical Chemistry*, **74**, 841–7.

64 Parak, W.J., Pellegrino, T. and Plank, C. (2005) Labelling of cells with quantum dots. *Nanotechnology*, **16**, R9–25.

65 Ghazani, A.A., Lee, J.A., Klostranec, J., Xiang, Q., Dacosta, R.S., Wilson, B.C., Tsao, M.S. and Chan, W.C. (2006) High throughput quantification of protein expression of cancer antigens in tissue microarray using quantum dot nanocrystals. *Nano Letters*, **6**, 2881–6.

66 Xiao, Y., Gao, X., Gannot, G., Emmert-Buck, M.R., Srivastava, S., Wagner, P.D., Amos, M.D. and Barker, P.E. (2008) Quantitation of HER2 and telomerase biomarkers in solid tumors with IgY antibodies and nanocrystal detection. *International Journal of Cancer*, **122**, 2178–86.

67 Caldwell, M.L., Moffitt, R.A., Liu, J., Parry, R., Sharma, Y. and Wang, M.D. (2008) Simple quantification of multiplexed Quantum Dot staining in clinical tissue samples. *Conference Proceedings IEEE Engineering in Medicine and Biology Society*, **2008**, 1907–10.

68 Zajac, A., Song, D., Qian, W. and Zhukov, T. (2007) Protein microarrays and quantum dot probes for early cancer detection. *Colloids and Surfaces B, Biointerfaces*, **58**, 309–14.

69 Gokarna, A., Jin, L.H., Hwang, J.S., Cho, Y.H., Lim, Y.T., Chung, B.H., Youn, S.H., Choi, D.S. and Lim, J.H. (2008)

Quantum dot-based protein micro- and nanoarrays for detection of prostate cancer biomarkers. *Proteomics*, **8**, 1809–18.

70 Li-Shishido, S., Watanabe, T.M., Tada, H., Higuchi, H. and Ohuchi, N. (2006) Reduction in nonfluorescence state of quantum dots on an immunofluorescence staining. *Biochemical and Biophysical Research Communications*, **351**, 7–13.

71 Itoh, J. and Osamura, R.Y. (2007) Quantum dots for multicolor tumor pathology and multispectral imaging. *Methods in Molecular Biology*, **374**, 29–42.

72 Sun, J., Zhu, M.Q., Fu, K., Lewinski, N. and Drezek, R.A. (2007) Lead sulfide near-infrared quantum dot bioconjugates for targeted molecular imaging. *International Journal of Nanomedicine*, **2**, 235–40.

73 Xu, H., Peng, J., Tang, H.W., Li, Y., Wu, Q.S., Zhang, Z.L., Zhou, G., Chen, C. and Li, Y. (2009) Hadamard transform spectral microscopy for single cell imaging using organic and quantum dot fluorescent probes. *Analyst*, **134**, 504–11.

74 Wang, H.Z., Wang, H.Y., Liang, R.Q. and Ruan, K.C. (2004) Detection of tumor marker CA125 in ovarian carcinoma using quantum dots. *Acta Biochimica et Biophysica Sinica (Shanghai)*, **36**, 681–6.

75 Shi, C., Zhou, G., Zhu, Y., Su, Y., Cheng, T., Zhau, H.E. and Chung, L.W. (2008) Quantum dots-based multiplexed immunohistochemistry of protein expression in human prostate cancer cells. *European Journal of Histochemistry*, **52**, 127–34.

76 Bostick, R.M., Kong, K.Y., Ahearn, T.U., Chaudry, Q., Cohen, V. and Wang, M.D. (2006) Detecting and quantifying biomarkers of risk for colorectal cancer using quantum dots and novel image analysis algorithms. *Conference Proceedings IEEE Engineering in Medicine and Biology Society*, **1**, 3313–16.

77 Fountaine, T.J., Wincovitch, S.M., Geho, D.H., Garfield, S.H. and Pittaluga, S. (2006) Multispectral imaging of clinically relevant cellular targets in tonsil and lymphoid tissue using semiconductor quantum dots. *Modern Pathology*, **19**, 1181–191.

78 Sweeney, E., Ward, T.H., Gray, N., Womack, C., Jayson, G., Hughes, A., Dive, C. and Byers, R. (2008) Quantitative multiplexed quantum dot immunohistochemistry. *Biochemical and Biophysical Research Communications*, **374**, 181–6.

79 Kaul, Z., Yaguchi, T., Kaul, S.C., Hirano, T., Wadhwa, R. and Taira, K. (2003) Mortalin imaging in normal and cancer cells with quantum dot immuno-conjugates. *Cell Research*, **13**, 503–7.

80 Li, Z., Wang, K., Tan, W., Li, J., Fu, Z., Ma, C., Li, H., He, X. and Liu, J. (2006) Immunofluorescent labeling of cancer cells with quantum dots synthesized in aqueous solution. *Analytical Biochemistry*, **354**, 169–74.

81 Yang, D., Chen, Q., Wang, W. and Xu, S. (2008) Direct and indirect immunolabelling of HeLa cells with quantum dots. *Luminescence*, **23**, 169–74.

82 Chatterjee, U., Bose, P.P., Dey, S., Singh, T.P. and Chatterjee, B.P. (2008) Antiproliferative effect of T/Tn specific Artocarpus lakoocha agglutinin (ALA) on human leukemic cells (Jurkat, U937, K562) and their imaging by QD-ALA nanoconjugate. *Glycoconjugate Journal*, **25**, 741–52.

83 Kaul, Z., Yaguchi, T., Kaul, S.C. and Wadhwa, R. (2006) Quantum dot-based protein imaging and functional significance of two mitochondrial chaperones in cellular senescence and carcinogenesis. *Annals of the New York Academy of Sciences*, **1067**, 469–73.

84 Xiao, Y., Gao, X., Maragh, S., Telford, W.G. and Tona, A. (2009) Cell lines as candidate reference materials for quality control of HER2 amplification and expression assays in breast cancer. *Clinical Chemistry*, **55**, 1307–15.

85 Karwa, A., Papazoglou, E., Pourrezaei, K., Tyagi, S. and Murthy, S. (2007) Imaging biomarkers of inflammation in situ with functionalized quantum dots in the dextran sodium sulfate (DSS) model of mouse colitis. *Inflammation Research*, **56**, 502–10.

86 Xiao, Y., Telford, W.G., Ball, J.C., Locascio, L.E. and Barker, P.E. (2005)

Semiconductor nanocrystal conjugates, FISH and pH. *Nature Methods*, **2**, 723.

87 Xiao, Y. and Barker, P.E. (2004) Semiconductor nanocrystal probes for human metaphase chromosomes. *Nucleic Acids Research*, **32**, e28.

88 Chan, P., Yuen, T., Ruf, F., Gonzalez-Maeso, J. and Sealfon, S.C. (2005) Method for multiplex cellular detection of mRNAs using quantum dot fluorescent in situ hybridization. *Nucleic Acids Research*, **33**, e161.

89 Bentolila, L.A. and Weiss, S. (2006) Single-step multicolor fluorescence in situ hybridization using semiconductor quantum dot-DNA conjugates. *Cell Biochemistry and Biophysics*, **45**, 59–70.

90 Jiang, Z., Li, R., Todd, N.W., Stass, S.A. and Jiang, F. (2007) Detecting genomic aberrations by fluorescence in situ hybridization with quantum dots-labeled probes. *Journal of Nanoscience and Nanotechnology*, **7**, 4254–9.

91 Byers, R.J., Di Vizio, D., O'Connell, F., Tholouli, E., Levenson, R.M., Gossage, K., Twomey, D., Yang, Y., Benedettini, E., Rose, J., Ligon, K.L., Finn, S.P., Golub, T.R. and Loda, M. (2007) Semiautomated multiplexed quantum dot-based in situ hybridization and spectral deconvolution. *The Journal of Molecular Diagnostics*, **9**, 20–9.

92 Minet, O., Dressler, C. and Beuthan, J. (2004) Heat stress induced redistribution of fluorescent quantum dots in breast tumor cells. *Journal of Fluorescence*, **14**, 241–7.

93 Nida, D.L., Rahman, M.S., Carlson, K.D., Richards-Kortum, R. and Follen, M. (2005) Fluorescent nanocrystals for use in early cervical cancer detection. *Gynecologic Oncology*, **99**, S89–94.

94 Rahman, M., Abd-El-Barr, M., Mack, V., Tkaczyk, T., Sokolov, K., Richards-Kortum, R. and Descour, M. (2005) Optical imaging of cervical pre-cancers with structured illumination: an integrated approach. *Gynecologic Oncology*, **99**, S112–15.

95 Lidke, D.S., Lidke, K.A., Rieger, B., Jovin, T.M. and Arndt-Jovin, D.J. (2005) Reaching out for signals: filopodia sense EGF and respond by directed retrograde transport of activated receptors. *The Journal of Cell Biology*, **170**, 619–26.

96 Lidke, D.S., Nagy, P., Jovin, T.M. and Arndt-Jovin, D.J. (2007) Biotin-ligand complexes with streptavidin quantum dots for *in vivo* cell labeling of membrane receptors. *Methods in Molecular Biology*, **374**, 69–79.

97 Young, S.H. and Rozengurt, E. (2006) Qdot nanocrystal conjugates conjugated to bombesin or ANG II label the cognate G protein-coupled receptor in living cells. *American Journal of Physiology Cell Physiology*, **290**, C728–32.

98 Chu, T.C., Shieh, F., Lavery, L.A., Levy, M., Richards-Kortum, R., Korgel, B.A. and Ellington, A.D. (2006) Labeling tumor cells with fluorescent nanocrystal-aptamer bioconjugates. *Biosensors & Bioelectronics*, **21**, 1859–66.

99 Liu, T.C., Wang, J.H., Wang, H.Q., Zhang, H.L., Zhang, Z.H., Hua, X.F., Cao, Y.C., Zhao, Y.D. and Luo, Q.M. (2007) Bioconjugate recognition molecules to quantum dots as tumor probes. *Journal of Biomedical Materials Research Part A*, **83**, 1209–16.

100 Cheng, C.M., Chu, P.Y., Chuang, K.H., Roffler, S.R., Kao, C.H., Tseng, W.L., Shiea, J., Chang, W.D., Su, Y.C., Chen, B.M., Wang, Y.M. and Cheng, T.L. (2009) Hapten-derivatized nanoparticle targeting and imaging of gene expression by multimodality imaging systems. *Cancer Gene Therapy*, **16**, 83–90.

101 Grecco, H.E., Lidke, K.A., Heintzmann, R., Lidke, D.S., Spagnuolo, C., Martinez, O.E., Jares-Erijman, E.A. and Jovin, T.M. (2004) Ensemble and single particle photophysical properties (two-photon excitation, anisotropy, FRET, lifetime, spectral conversion) of commercial quantum dots in solution and in live cells. *Microscopy Research and Technique*, **65**, 169–79.

102 Watanabe, T.M. and Higuchi, H. (2007) Stepwise movements in vesicle transport of HER2 by motor proteins in living cells. *Biophysical Journal*, **92**, 4109–20.

103 Qian, J., Yong, K.T., Roy, I., Ohulchanskyy, T.Y., Bergey, E.J., Lee, H.H., Tramposch, K.M., He, S., Maitra, A. and Prasad, P.N. (2007) Imaging

pancreatic cancer using surface-functionalized quantum dots. *The Journal of Physical Chemistry B*, **111**, 6969–72.

104 Watanabe, T.M., Sato, T., Gonda, K. and Higuchi, H. (2007) Three-dimensional nanometry of vesicle transport in living cells using dual-focus imaging optics. *Biochemical and Biophysical Research Communications*, **359**, 1–7.

105 Erogbogbo, F., Yong, K.T., Roy, I., Xu, G., Prasad, P.N. and Swihart, M.T. (2008) Biocompatible luminescent silicon quantum dots for imaging of cancer cells. *ACS Nano*, **2**, 873–8.

106 Tekle, C., Deurs, B., Sandvig, K. and Iversen, T.G. (2008) Cellular trafficking of quantum dot-ligand bioconjugates and their induction of changes in normal routing of unconjugated ligands. *Nano Letters*, **8**, 1858–65.

107 Weng, K.C., Noble, C.O., Papahadjopoulos-Sternberg, B., Chen, F.F., Drummond, D.C., Kirpotin, D.B., Wang, D., Hom, Y.K., Hann, B. and Park, J.W. (2008) Targeted tumor cell internalization and imaging of multifunctional quantum dot-conjugated immunoliposomes *in vitro* and *in vivo*. *Nano Letters*, **8**, 2851–7.

108 Schroeder, J.E., Shweky, I., Shmeeda, H., Banin, U. and Gabizon, A. (2007) Folate-mediated tumor cell uptake of quantum dots entrapped in lipid nanoparticles. *Journal of Controlled Release*, **124**, 28–34.

109 Pellegrino, T., Parak, W.J., Boudreau, R., Le Gros, M.A., Gerion, D., Alivisatos, A.P. and Larabell, C.A. (2003) Quantum dot-based cell motility assay. *Differentiation*, **71**, 542–8.

110 Gu, W., Pellegrino, T., Parak, W.J., Boudreau, R., Le Gros, M.A., Gerion, D., Alivisatos, A.P. and Larabell, C.A. (2005) Quantum-dot-based cell motility assay. *Science's STKE*, **2005**, l5.

111 Gu, W., Pellegrino, T., Parak, W.J., Boudreau, R., Le Gros, M.A., Alivisatos, A.P. and Larabell, C.A. (2007) Measuring cell motility using quantum dot probes. *Methods in Molecular Biology*, **374**, 125–31.

112 Clift, M.J., Rothen-Rutishauser, B., Brown, D.M., Duffin, R., Donaldson, K., Proudfoot, L., Guy, K. and Stone, V. (2008) The impact of different nanoparticle surface chemistry and size on uptake and toxicity in a murine macrophage cell line. *Toxicology and Applied Pharmacology*, **232**, 418–27.

113 Barua, S. and Rege, K. (2009) Cancer-cell-phenotype-dependent differential intracellular trafficking of unconjugated quantum dots. *Small*, **5**, 370–6.

114 Voura, E.B., Jaiswal, J.K., Mattoussi, H. and Simon, S.M. (2004) Tracking metastatic tumor cell extravasation with quantum dot nanocrystals and fluorescence emission-scanning microscopy, *Nature Medicine*, **10**, 993–8.

115 Chang, C.F., Chen, C.Y., Chang, F.H., Tai, S.P., Chen, C.Y., Yu, C.H., Tseng, Y.B., Tsai, T.H., Liu, I.S., Su, W.F. and Sun, C.K. (2008) Cell tracking and detection of molecular expression in live cells using lipid-enclosed CdSe quantum dots as contrast agents for epi-third harmonic generation microscopy. *Optics Express*, **16**, 9534–48.

116 Yoo, J., Kambara, T., Gonda, K. and Higuchi, H. (2008) Intracellular imaging of targeted proteins labeled with quantum dots. *Experimental Cell Research*, **314**, 3563–9.

117 Nan, X., Sims, P.A., Chen, P. and Xie, X.S. (2005) Observation of individual microtubule motor steps in living cells with endocytosed quantum dots. *The Journal of Physical Chemistry B*, **109**, 24220–4.

118 Wylie, P.G. (2007) Multiple cell lines using quantum dots. *Methods in Molecular Biology*, **374**, 113–23.

119 Xue, F.L., Chen, J.Y., Guo, J., Wang, C.C., Yang, W.L., Wang, P.N. and Lu, D.R. (2007) Enhancement of intracellular delivery of CdTe quantum dots (QDs) to living cells by Tat conjugation. *Journal of Fluorescence*, **17**, 149–54.

120 Garon, E.B., Marcu, L., Luong, Q., Tcherniantchouk, O., Crooks, G.M. and Koeffler, H.P. (2007) Quantum dot labeling and tracking of human leukemic, bone marrow and cord blood cells. *Leukemia Research*, **31**, 643–51.

121 Chen, B., Liu, Q., Zhang, Y., Xu, L. and Fang, X. (2008) Transmembrane delivery of the cell-penetrating peptide

conjugated semiconductor quantum dots. *Langmuir*, **24**, 11866–71.
122 Chen, A.K., Behlke, M.A. and Tsourkas, A. (2007) Avoiding false-positive signals with nuclease-vulnerable molecular beacons in single living cells. *Nucleic Acids Research*, **35**, e105.
123 Kaul, Z., Yaguchi, T., Harada, J.I., Ikeda, Y., Hirano, T., Chiura, H.X., Kaul, S.C. and Wadhwa, R. (2007) An antibody-conjugated internalizing quantum dot suitable for long-term live imaging of cells. *Biochemistry and Cell Biology*, **85**, 133–40.
124 Kaul, Z., Yaguchi, T., Chiura, H.X., Kaul, S.C. and Wadhwa, R. (2007) Quantum dot-based mortalin staining as a visual assay for detection of induced senescence in cancer cells. *Annals of the New York Academy of Sciences*, **1100**, 368–72.
125 Chen, L.D., Liu, J., Yu, X.F., He, M., Pei, X.F., Tang, Z.Y., Wang, Q.Q., Pang, D.W. and Li, Y. (2008) The biocompatibility of quantum dot probes used for the targeted imaging of hepatocellular carcinoma metastasis. *Biomaterials*, **29**, 4170–6.
126 Bidlingmaier, S., He, J., Wang, Y., An, F., Feng, J., Barbone, D., Gao, D., Franc, B., Broaddus, V.C. and Liu, B. (2009) Identification of MCAM/CD146 as the target antigen of a human monoclonal antibody that recognizes both epithelioid and sarcomatoid types of mesothelioma. *Cancer Research*, **69**, 1570–7.
127 Kim, B.Y., Jiang, W., Oreopoulos, J., Yip, C.M., Rutka, J.T. and Chan, W.C. (2008) Biodegradable quantum dot nanocomposites enable live cell labeling and imaging of cytoplasmic targets. *Nano Letters*, **8**, 3887–92.
128 Yezhelyev, M.V., Qi, L., O'Regan, R.M., Nie, S. and Gao, X. (2008) Proton-sponge coated quantum dots for siRNA delivery and intracellular imaging. *Journal of the American Chemical Society*, **130**, 9006–12.
129 Zhang, Y., So, M.K. and Rao, J. (2006) Protease-modulated cellular uptake of quantum dots. *Nano Letters*, **6**, 1988–92.
130 Stroh, M., Zimmer, J.P., Duda, D.G., Levchenko, T.S., Cohen, K.S., Brown, E.B., Scadden, D.T., Torchilin, V.P., Bawendi, M.G., Fukumura, D. and Jain, R.K. (2005) Quantum dots spectrally distinguish multiple species within the tumor milieu *in vivo*. *Nature Medicine*, **11**, 678–82.
131 Estrada, C.R., Salanga, M., Bielenberg, D.R., Harrell, W.B., Zurakowski, D., Zhu, X., Palmer, M.R., Freeman, M.R. and Adam, R.M. (2006) Behavioral profiling of human transitional cell carcinoma ex vivo. *Cancer Research*, **66**, 3078–86.
132 Morgan, N.Y., English, S., Chen, W., Chernomordik, V., Russo, A., Smith, P.D. and Gandjbakhche, A. (2005) Real time *in vivo* non-invasive optical imaging using near-infrared fluorescent quantum dots. *Academic Radiology*, **12**, 313–23.
133 Cai, W., Shin, D.W., Chen, K., Gheysens, O., Cao, Q., Wang, S.X., Gambhir, S.S. and Chen, X. (2006) Peptide-labeled near-infrared quantum dots for imaging tumor vasculature in living subjects. *Nano Letters*, **6**, 669–76.
134 Smith, B.R., Cheng, Z., De, A., Koh, A.L., Sinclair, R. and Gambhir, S.S. (2008) Real-time intravital imaging of RGD-quantum dot binding to luminal endothelium in mouse tumor neovasculature. *Nano Letters*, **8**, 2599–606.
135 Tanaka, E., Choi, H.S., Fujii, H., Bawendi, M.G. and Frangioni, J.V. (2006) Image-guided oncologic surgery using invisible light: completed pre-clinical development for sentinel lymph node mapping. *Annals of Surgical Oncology*, **13**, 1671–81.
136 Ballou, B., Ernst, L.A., Andreko, S., Harper, T., Fitzpatrick, J.A., Waggoner, A.S. and Bruchez, M.P. (2007) Sentinel lymph node imaging using quantum dots in mouse tumor models. *Bioconjugate Chemistry*, **18**, 389–96.
137 Takeda, M., Tada, H., Higuchi, H., Kobayashi, Y., Kobayashi, M., Sakurai, Y., Ishida, T. and Ohuchi, N. (2008) *In vivo* single molecular imaging and sentinel node navigation by nanotechnology for molecular targeting drug-delivery systems and tailor-made medicine. *Breast Cancer*, **15**, 145–52.

138 Hama, Y., Koyama, Y., Urano, Y., Choyke, P.L. and Kobayashi, H. (2007) Simultaneous two-color spectral fluorescence lymphangiography with near infrared quantum dots to map two lymphatic flows from the breast and the upper extremity. *Breast Cancer Research Treatment*, **103**, 23–8.

139 Kobayashi, H., Hama, Y., Koyama, Y., Barrett, T., Regino, C.A., Urano, Y. and Choyke, P.L. (2007) Simultaneous multicolor imaging of five different lymphatic basins using quantum dots. *Nano Letters*, **7**, 1711–16.

140 Yang, L., Mao, H., Wang, Y.A., Cao, Z., Peng, X., Wang, X., Duan, H., Ni, C., Yuan, Q., Adams, G., Smith, M.Q., Wood, W.C., Gao, X. and Nie, S. (2009) Single chain epidermal growth factor receptor antibody conjugated nanoparticles for *in vivo* tumor targeting and imaging. *Small*, **5**, 235–43.

141 Yu, X., Chen, L., Li, K., Li, Y., Xiao, S., Luo, X., Liu, J., Zhou, L., Deng, Y., Pang, D. and Wang, Q. (2007) Immunofluorescence detection with quantum dot bioconjugates for hepatoma *in vivo*. *Journal of Biomedical Optics*, **12**, 014008.

142 Tada, H., Higuchi, H., Wanatabe, T.M. and Ohuchi, N. (2007) *In vivo* real-time tracking of single quantum dots conjugated with monoclonal anti-HER2 antibody in tumors of mice. *Cancer Research*, **67**, 1138–44.

143 Diagaradjane, P., Orenstein-Cardona, J.M., Colón-Casasnovas, N.E., Deorukhkar, A., Shentu, S., Kuno, N., Schwartz, D.L., Gelovani, J.G. and Krishnan, S. (2008) Imaging epidermal growth factor receptor expression *in vivo*: pharmacokinetic and biodistribution characterization of a bioconjugated quantum dot nanoprobe. *Clinical Cancer Research*, **14**, 731–41.

144 Muhammad, O., Popescu, A. and Toms, S.A. (2007) Macrophage-mediated colocalization of quantum dots in experimental glioma. *Methods in Molecular Biology*, **374**, 161–71.

145 Cai, W., Chen, K., Li, Z.B., Gambhir, S.S. and Chen, X. (2007) Dual-function probe for PET and near-infrared fluorescence imaging of tumor vasculature. *Journal of Nuclear Medicine*, **48**, 1862–70.

146 Chen, K., Li, Z.B., Wang, H., Cai, W. and Chen, X. (2008) Dual-modality optical and positron emission tomography imaging of vascular endothelial growth factor receptor on tumor vasculature using quantum dots. *European Journal of Nuclear Medicine and Molecular Imaging*, **35**, 2235–44.

147 van Tilborg, G.A., Mulder, W.J., Chin, P.T., Storm, G., Reutelingsperger, C.P., Nicolay, K. and Strijkers, G.J. (2006) Annexin A5-conjugated quantum dots with a paramagnetic lipidic coating for the multimodal detection of apoptotic cells. *Bioconjugate Chemistry*, **17**, 865–8.

148 Oostendorp, M., Douma, K., Hackeng, T.M., Dirksen, A., Post, M.J., van Zandvoort, M.A. and Backes, W.H. (2008) Quantitative molecular magnetic resonance imaging of tumor angiogenesis using cNGR-labeled paramagnetic quantum dots. *Cancer Research*, **68**, 7676–83.

149 Bagalkot, V., Zhang, L., Levy-Nissenbaum, E., Jon, S., Kantoff, P.W., Langer, R. and Farokhzad, O.C. (2007) Quantum dot-aptamer conjugates for synchronous cancer imaging, therapy, and sensing of drug delivery based on bi-fluorescence resonance energy transfer. *Nano Letters*, **7**, 3065–70.

150 Derfus, A.M., Chen, A.A., Min, D.H., Ruoslahti, E. and Bhatia, S.N. (2007) Targeted quantum dot conjugates for siRNA delivery. *Bioconjugate Chemistry*, **18**, 1391–6.

151 Pan, J. and Feng, S.S. (2009) Targeting and imaging cancer cells by folate-decorated, quantum dots (QDs)-loaded nanoparticles of biodegradable polymers. *Biomaterials*, **30**, 1176–83.

152 Hyun, B.R., Chen, H., Rey, D.A., Wise, F.W. and Batt, C.A. (2007) Near-infrared fluorescence imaging with water-soluble lead salt quantum dots. *The Journal of Physical Chemistry B*, **111**, 5726–30.

153 Liu, S., Lee, C.M., Wang, S. and Lu, D.R. (2006) A new bioimaging carrier for fluorescent quantum dots: phospholipid nanoemulsion mimicking natural lipoprotein core. *Drug Delivery*, **13**, 159–64.

154 Ballou, B., Ernst, L.A. and Waggoner, A.S. (2005) Fluorescence imaging of tumors *in vivo*. *Current Medicinal Chemistry*, **12**, 795–805.

155 Rao, J., Dragulescu-Andrasi, A. and Yao, H. (2007) Fluorescence imaging *in vivo*: recent advances. *Current Opinion in Biotechnology*, **18**, 17–25.

156 Cheong, W.F., Prahl, S.A. and Welch, A.J. (1990) A review of the optical properties of biological tissues. *IEEE Journal of Quantum Electronics*, **26**, 2166–95.

157 Weissleder, R. (2001) A clearer vision for *in vivo* imaging. *Nature Biotechnology*, **19**, 316–17.

158 Mansfield, J.R., Gossage, K.W., Hoyt, C.C. and Levenson, R.M. (2005) Autofluorescence removal, multiplexing, and automated analysis methods for in-vivo fluorescence imaging. *Journal of Biomedical Optics*, **10**, 41207.

159 Gao, X. (2007) Multifunctional quantum dots for cellular and molecular imaging. *Conference Proceedings IEEE Engineering in Medicine and Biology Society*, **2007**, 524–5.

160 True, L.D. and Gao, X. (2007) Quantum dots for molecular pathology: their time has arrived. *The Journal of Molecular Diagnostics*, **9**, 7–11.

161 Jain, R.K. and Duda, D.G. (2003) Role of bone marrow-derived cells in tumor angiogenesis and treatment. *Cancer Cell*, **3**, 515–16.

162 Das, B., Tsuchida, R., Malkin, D., Koren, G., Baruchel, S. and Yeger, H. (2008) Hypoxia enhances tumor stemness by increasing the invasive and tumorigenic side population fraction. *Stem Cells*, **26**, 1818–30.

163 Duan, H. and Nie, S. (2007) Cell-penetrating quantum dots based on multivalent and endosome-disrupting surface coatings. *Journal of the American Chemical Society*, **129**, 3333–8.

164 Al-Jamal, W.T., Al-Jamal, K.T., Bomans, P.H., Frederik, P.M. and Kostarelos, K. (2008) Functionalized-quantum-dot-liposome hybrids as multimodal nanoparticles for cancer. *Small*, **4**, 1406–15.

165 Larson, D.R., Zipfel, W.R., Williams, R.M., Clark, S.W., Bruchez, M.P., Wise, F.W. and Webb, W.W. (2003) Water-soluble quantum dots for multiphoton fluorescence imaging *in vivo*. *Science*, **300**, 1434–6.

166 Lim, Y.T., Kim, S., Nakayama, A., Stott, N.E., Bawendi, M.G. and Frangioni, J.V. (2003) Selection of quantum dot wavelengths for biomedical assays and imaging. *Molecular Imaging*, **2**, 50–64.

167 Smith, J.D., Fisher, G.W., Waggoner, A.S. and Campbell, P.G. (2007) The use of quantum dots for analysis of chick CAM vasculature. *Microvascular Research*, **73**, 75–83.

168 Jayagopal, A., Russ, P.K. and Haselton, F.R. (2007) Surface engineering of quantum dots for *in vivo* vascular imaging. *Bioconjugate Chemistry*, **18**, 1424–33.

169 Cai, W. and Chen, X. (2008) Preparation of peptide-conjugated quantum dots for tumor vasculature-targeted imaging. *Nature Protocols*, **3**, 89–96.

170 Curnis, F., Sacchi, A., Gasparri, A., Longhi, R., Bachi, A., Doglioni, C., Bordignon, C., Traversari, C., Rizzardi, G.P. and Corti, A. (2008) Isoaspartate-glycine-arginine a new tumor vasculature-targeting motif. *Cancer Research*, **68**, 7073–82.

171 Schulze, T., Bembenek, A. and Schlag, P.M. (2004) Sentinel lymph node biopsy progress in surgical treatment of cancer. *Langenbeck's Archives of Surgery*, **389**, 532–50.

172 Morton, D.L., Wen, D.R., Wong, J.H., Economou, J.S., Cagle, L.A., Storm, F.K., Foshag, L.J. and Cochran, A.J. (1992) Technical details of intraoperative lymphatic mapping for early stage melanoma. *Archives of Surgery*, **127**, 392–9.

173 Kim, S., Lim, Y.T., Soltesz, E.G., De Grand, A.M., Lee, J., Nakayama, A., Parker, J.A., Mihaljevic, T., Laurence, R.G., Dor, D.M., Cohn, L.H., Bawendi, M.G. and Frangioni, J.V. (2004) Near-infrared fluorescent type II quantum dots for sentinel lymph node mapping. *Nature Biotechnology*, **22**, 93–7.

174 Soltesz, E.G., Kim, S., Laurence, R.G., De Grand, A.M., Parungo, C.P., Dor, D.M., Cohn, L.H., Bawendi, M.G., Frangioni, J.V. and Mihaljevic, T. (2005)

Intraoperative sentinel lymph node mapping of the lung using near-infrared fluorescent quantum dots. *The Annals of Thoracic Surgery*, **79**, 269–77.

175 Parungo, C.P., Ohnishi, S., Kim, S.W., Kim, S., Laurence, R.G., Soltesz, E.G., Chen, F.Y., Colson, Y.L., Cohn, L.H., Bawendi, M.G. and Frangioni, J.V. (2005) Intraoperative identification of esophageal sentinel lymph nodes with near-infrared fluorescence imaging. *The Journal of Thoracic and Cardiovascular Surgery*, **129**, 844–50.

176 Parungo, C.P., Colson, Y.L., Kim, S.W., Kim, S., Cohn, L.H., Bawendi, M.G. and Frangioni, J.V. (2005) Sentinel lymph node mapping of the pleural space. *Chest*, **127**, 1799–804.

177 Ohnishi, S., Lomnes, S.J., Laurence, R.G., Gogbashian, A., Mariani, G. and Frangioni, J.V. (2005) Organic alternatives to quantum dots for intraoperative near-infrared fluorescent sentinel lymph node mapping. *Molecular Imaging*, **4**, 172–81.

178 Soltesz, E.G., Kim, S., Kim, S.W., Laurence, R.G., De Grand, A.M., Parungo, C.P., Cohn, L.H., Bawendi, M.G. and Frangioni, J.V. (2006) Sentinel lymph node mapping of the gastrointestinal tract by using invisible light. *Annals of Surgical Oncology*, **13**, 386–96.

179 Robe, A., Pic, E., Lassalle, H.P., Bezdetnaya, L., Guillemin, F. and Marchal, F. (2008) Quantum dots in axillary lymph node mapping: biodistribution study in healthy mice. *BMC Cancer*, **8**, 111.

180 Maeda, H., Wu, J., Sawa, T., Matsumura, Y. and Hori, K. (2000) Tumor vascular permeability and the EPR effect in macromolecular therapeutics: a review. *Journal of Controlled Release*, **65**, 271–84.

181 Gao, X., Chung, L.W. and Nie, S. (2007) Quantum dots for *in vivo* molecular and cellular imaging. *Methods in Molecular Biology*, **374**, 135–45.

182 Inoue, Y., Izawa, K., Yoshikawa, K., Yamada, H., Tojo, A. and Ohtomo, K. (2007) *In vivo* fluorescence imaging of the reticuloendothelial system using quantum dots in combination with bioluminescent tumour monitoring. *European Journal of Nuclear Medicine and Molecular Imaging*, **34**, 2048–56.

183 Schipper, M.L., Iyer, G., Koh, A.L., Cheng, Z., Ebenstein, Y., Aharoni, A., Keren, S., Bentolila, L.A., Li, J., Rao, J., Chen, X., Banin, U., Wu, A.M., Sinclair, R., Weiss, S. and Gambhir, S.S. (2009) Particle size, surface coating, and PEGylation influence the biodistribution of quantum dots in living mice. *Small*, **5**, 126–34.

184 Corot, C., Petry, K.G., Trivedi, R., Saleh, A., Jonkmanns, C., Le Bas, J.F., Blezer, E., Rausch, M., Brochet, B., Foster-Gareau, P., Balériaux, D., Gaillard, S. and Dousset, V. (2004) Macrophage imaging in central nervous system and in carotid atherosclerotic plaque using ultrasmall superparamagnetic iron oxide in magnetic resonance imaging. *Investigative Radiology*, **39**, 619–25.

185 Devi, G.R. (2006) siRNA-based approaches in cancer therapy. *Cancer Gene Therapy*, **13**, 819–29.

186 Hoet, P.H., Brüske-Hohlfeld, I. and Salata, O.V. (2004) Nanoparticles – known and unknown health risks. *Journal of Nanobiotechnology*, **2**, 12.

187 Singh, S. and Nalwa, H.S. (2007) Nanotechnology and health safety – toxicity and risk assessments of nanostructured materials on human health. *Journal of Nanoscience and Nanotechnology*, **7**, 3048–70.

188 Hardman, R. (2006) A toxicologic review of quantum dots: toxicity depends on physicochemical and environmental factors. *Environmental Health Perspectives*, **114**, 165–72.

189 Derfus, A.M., Chan, W.C. and Bhatia, S.N. (2004) Probing the cytotoxicity of semiconductor quantum dots. *Nano Letters*, **4**, 11–18.

190 Pradhan, N., Goorskey, D., Thessing, J. and Peng, X. (2005) An alternative of CdSe nanocrystal emitters: pure and tunable impurity emissions in ZnSe nanocrystals. *Journal of the American Chemical Society*, **127**, 17586–7.

191 Yu, W.W., Chang, E., Drezek, R. and Colvin, V.L. (2006) Water-soluble quantum dots for biomedical applications. *Biochemical and Biophysical Research Communications*, **348**, 781–6.

192 Ballou, B., Lagerholm, B.C., Ernst, L.A., Bruchez, M.P. and Waggoner, A.S. (2004) Noninvasive imaging of quantum dots in mice. *Bioconjugate Chemistry*, **15**, 79–86.

193 Hoshino, A., Fujioka, K., Oku, T., Suga, M., Sasaki, Y.F., Ohta, T., Yasuhara, M., Suzuki, K. and Yamamoto, K. (2004) Physicochemical properties and cellular toxicity of nanocrystal quantum dots depend on their surface modification. *Nano Letters*, **4**, 2163–9.

194 Aldana, J., Wang, Y.A. and Peng, X. (2001) Photochemical instability of CdSe nanocrystals coated by hydrophilic thiols. *Journal of the American Chemical Society*, **123**, 8844–50.

195 Gerion, D., Pinaud, F., Williams, S.C., Parak, W.J., Zanchet, D., Weiss, S. and Alivisatos, A.P. (2001) Synthesis and properties of biocompatible water-soluble silica-coated CdSe/ZnS semiconductor quantum dots. *Journal of Physical Chemistry B*, **105**, 8861–71.

196 Zhang, T., Stilwell, J.L., Gerion, D., Ding, L., Elboudwarej, O., Cooke, P.A., Gray, J.W., Alivisatos, A.P. and Chen, F.F. (2006) Cellular effect of high doses of silica-coated quantum dot profiled with high throughput gene expression analysis and high content cellomics measurements. *Nano Letters*, **6**, 800–8.

197 Cho, S.J., Maysinger, D., Jain, M., Röder, B., Hackbarth, S. and Winnik, F.M. (2007) Long-term exposure to CdTe quantum dots causes functional impairments in live cells. *Langmuir*, **23**, 1974–80.

198 Lovri , J., Cho, S.J., Winnik, F.M. and Maysinger, D. (2005) Unmodified cadmium telluride quantum dots induce reactive oxygen species formation leading to multiple organelle damage and cell death. *Chemistry & Biology*, **12**, 1227–34.

199 Ipe, B.I., Lehnig, M. and Niemeyer, C.M. (2005) On the generation of free radical species from quantum dots. *Small*, **1**, 706–9.

200 Chan, W.H., Shiao, N.H. and Lu, P.Z. (2006) CdSe quantum dots induce apoptosis in human neuroblastoma cells via mitochondrial-dependent pathways and inhibition of survival signals. *Toxicology Letters*, **167**, 191–200.

201 Green, M. and Howman, E. (2005) Semiconductor quantum dots and free radical induced DNA nicking. *Chemical Communications (Cambridge, England)*, **1**, 121–3.

202 Ryman-Rasmussen, J.P., Riviere, J.E. and Monteiro-Riviere, N.A. (2007) Surface coatings determine cytotoxicity and irritation potential of quantum dot nanoparticles in epidermal keratinocytes. *Journal of Investigative Dermatology*, **127**, 143–53.

203 Wang, L., Nagesha, D.K., Selvarasah, S., Dokmeci, M.R. and Carrier, R.L. (2008) Toxicity of CdSe nanoparticles in Caco-2 cell cultures. *Journal of Nanobiotechnology*, **6**, 11.

204 Jaiswal, J.K., Goldman, E.R., Mattoussi, H. and Simon, S.M. (2004) Use of quantum dots for live cell imaging. *Nature Methods*, **1**, 73–8.

205 Shiohara, A., Hoshino, A., Hanaki, K., Suzuki, K. and Yamamoto, K. (2004) On the cyto-toxicity caused by quantum dots. *Microbiology and Immunology*, **48**, 669–75.

206 Fischer, H.C., Liu, L., Pang, K.S. and Chan, W.C.W. (2006) Pharmacokinetics of nanoscale quantum dots: *in vivo* distribution, sequestration, and clearance in the rat. *Advanced Functional Materials*, **16**, 1299–305.

207 Hsieh, S.C., Wang, F.F., Lin, C.S., Chen, Y.J., Hung, S.C. and Wang, Y.J. (2006) The inhibition of osteogenesis with human bone marrow mesenchymal stem cells by CdSe/ZnS quantum dot labels. *Biomaterials*, **27**, 1656–64.

208 Hsieh, S.C., Wang, F.F., Hung, S.C., Chen, Y.J. and Wang, Y.J. (2006) The internalized CdSe/ZnS quantum dots impair the chondrogenesis of bone marrow mesenchymal stem cells. *Journal of Biomedical Materials Research Part B, Applied Biomaterials*, **79**, 95–101.

209 Choi, A.O., Cho, S.J., Desbarats, J., Lovrić , J. and Maysinger, D. (2007) Quantum dot-induced cell death involves Fas upregulation and lipid peroxidation in human neuroblastoma cells. *Journal of Nanobiotechnology*, **5**, 1.